

Angiotensin II Analogues Encompassing 5,9- and 5,10-Fused Thiazabicycloalkane Tripeptide Mimetics

Petra Johannesson,[†] Gunnar Lindeberg,[†] Weimin Tong,[†] Adolf Gogoll,[‡] Barbro Synnergren,[§] Fred Nyberg,[§] Anders Karlén,[†] and Anders Hallberg^{*,†}

Department of Organic Pharmaceutical Chemistry, Uppsala University, Box 574, SE-751 23 Uppsala, Sweden,

Department of Organic Chemistry, Uppsala University, Box 531, SE-751 21 Uppsala, Sweden, and

Department of Biological Research on Drug Dependence, Uppsala University, Box 591, SE-751 24 Uppsala, Sweden

Received May 31, 1999

A simple experimental procedure on solid phase for the construction of new tripeptidic 5,9- and 5,10-fused thiazabicycloalkane scaffolds that adopt β -turns has been developed. This N-terminal-directed bicyclization, relying on masked aldehyde precursors derived from glutamic acid as key building blocks, provides a complement to the related bicyclization previously reported, where an aspartic acid-derived precursor was employed to induce cyclization toward the C-terminal end of the peptide. Thus, the regioselectivity of the bicyclization can be altered simply by varying the chain length of the incorporated aldehyde precursor. Four analogues of the hypertensive octapeptide angiotensin II, comprising the new scaffolds in the 3–5- and 5–7-positions, were synthesized. One of these conformationally constrained angiotensin II analogues exhibited AT₁ receptor affinity ($K_i = 750$ nM). Results from theoretical conformational analysis of model compounds of the bicyclic tripeptide mimetics are presented, and they demonstrate that subtle differences in geometry have a strong impact on the affinity to the AT₁ receptor.

Introduction

Determination of the bioactive conformations of biologically active peptides remains an exciting challenge. Linear peptides interconvert rapidly in solution between conformations which differ little in energy, and knowledge of a preferred solution conformation does not necessarily provide information regarding the receptor-bound conformation of the peptide. Insights into the topological requirements within a peptide–receptor complex are of the utmost importance in drug discovery programs, where often the conversion of peptides into nonpeptidic organic molecules, with high bioavailability and with retained biological activity, is the ultimate goal. To date, no three-dimensional structural data are available for peptides interacting with their G-protein-coupled receptor targets, and critical information of the receptor-bound conformation has to be gained in an indirect fashion. One strategy involves the introduction of conformational constraints, for example, by cyclization^{1,2} or by incorporation of secondary structure mimetics^{3–7} at selected sites of the peptide, to enforce important recognition elements into the correct regions of space.

This strategy has been successful in the search for the bioactive conformation of the hypertensive octapeptide angiotensin II (Ang II), **1** (Chart 1).^{8–15} Spear et al.⁹ have reported that displacement of Val³ and Ile⁵ in Ang II by Hcy³ and Hcy⁵ and subsequent oxidation furnished the potent agonist c[Hcy^{3,5}]Ang II, **2**. Conformational analysis and further synthetic elaborations involving the synthesis of the more constrained bicyclic agonist c[Sar¹, Hcy³, Mpt⁵]Ang II, **3** (Chart 1),¹¹ allowed

Nikiforovich and Marshall to postulate a model of the bioactive conformation of Ang II when binding to the AT₁ receptor.^{16,17} Further modifications, now in the 5–7 region of Ang II, provided the bicyclic analogue c[Sar¹, Hcy⁵, Mpc⁷]Ang II, **4**, which also has good binding affinity toward AT₁ receptors and exerts a partial agonistic effect.¹⁴ Our incorporation of γ -turn mimetics into the 3–5 region of Ang II required considerable synthetic efforts and resulted in an agonist, although 300-fold less potent than Ang II.¹⁵

There is a real need for new, complementary, flexible, and synthetically simple cyclization methods for peptides, which enforce conformational constraints and allow for fine-tuning of models of bioactive conformations. These methods should preferably be exploited prior to the initiation of the often tedious synthetic programs aimed at more complex organic scaffolds. Although several methods for the synthesis of constrained bicyclic *dipeptides*, including motifs mimicking β -turns, have appeared in the literature,^{18–23} reports on the corresponding bicyclic *tripeptides* with reverse turn-inducing properties are rare.

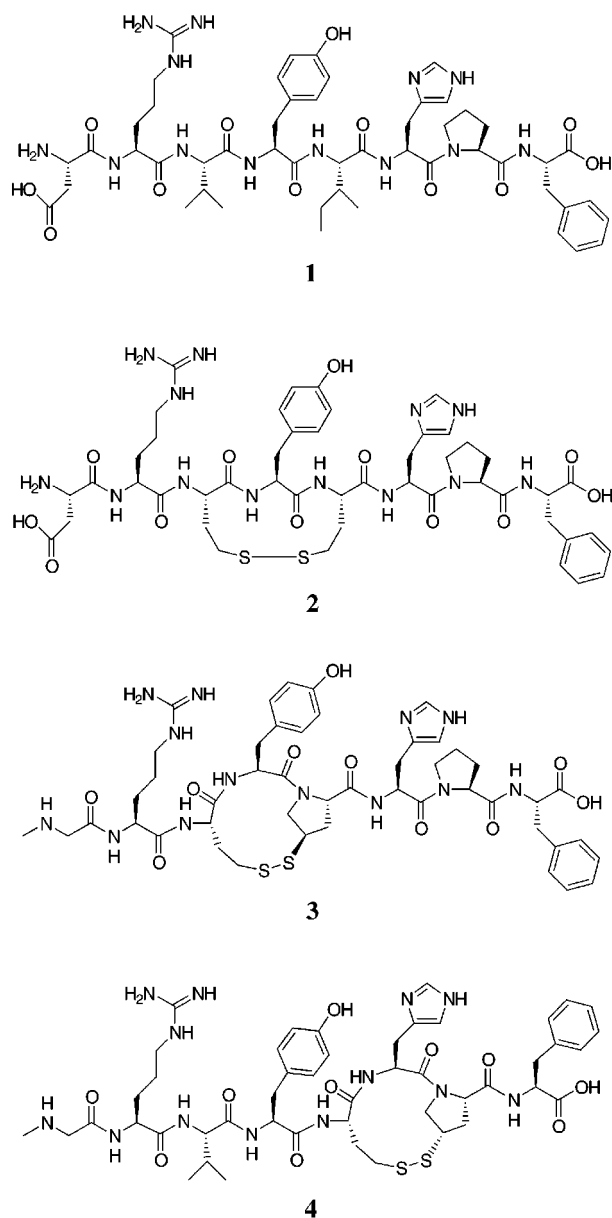
We have an interest in developing cyclization strategies that stabilize secondary structures, such as β -turns and γ -turns, in peptides. Previously, we have reported a procedure on solid phase for the preparation of a series of Ang II analogues encompassing the bicyclic tripeptide scaffolds **5** and **6** which have β -turn-inducing properties (Chart 2).²⁴ A masked ω -formyl α -amino acid derived from L-aspartic acid was used as building block, and a stereoselective C-terminal-directed bicyclization was achieved. The simplicity of the experimental procedure and the obvious potential of the bicyclization strategy for the construction of a diversity of constrained backbone scaffolds encouraged us to survey its applicability. We herein report that by employing building blocks

[†] Department of Organic Pharmaceutical Chemistry.

[‡] Department of Organic Chemistry.

[§] Department of Biological Research on Drug Dependence.

Chart 1

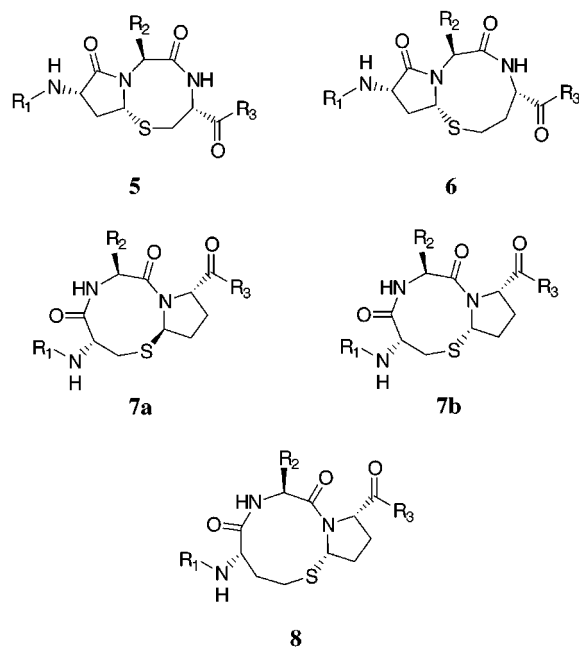


derived from L-glutamic acid as a substitute for L-aspartic acid, N-terminal-directed bicyclization can be accomplished providing the new tripeptidic scaffolds **7a**, **7b**, and **8** (Chart 2). We also report the binding affinities of four Ang II analogues encompassing the new scaffolds in the 3-5- and the 5-7-positions. Finally, we present the results from a theoretical conformational analysis of these scaffolds.

Results

Synthesis. Two alternative Fmoc-protected building blocks were prepared and thereafter incorporated into Ang II. The synthesis of the first, Fmoc-protected 5-hydroxyproline **12**, is outlined in Scheme 1. The *N*-Boc-protected aldehyde derived from glutamic acid has been reported to spontaneously cyclize to 5-hydroxyproline.²⁵ Initial experiments to prepare the aldehyde by controlled oxidation of the corresponding primary alcohol were unsuccessful and led to overoxidation to pyroglutamic acid.²⁵ The aldehyde therefore was prepared under reductive conditions via the Weinreb

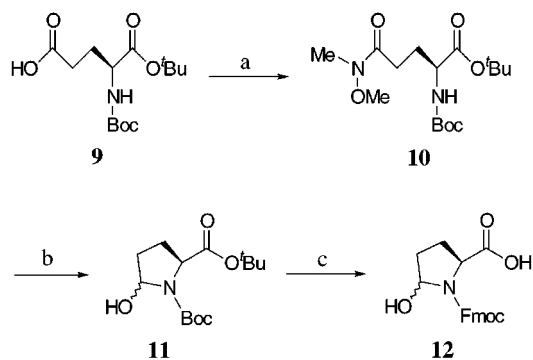
Chart 2



In Model Compounds: $R_1 = \text{CH}_3\text{CO}$

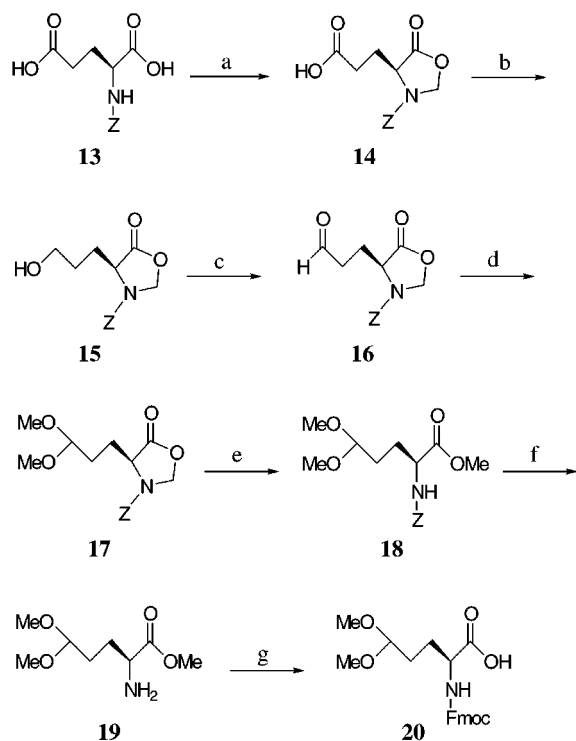
$R_2 = \text{CH}_3$

$R_3 = \text{NHCH}_3$

Scheme 1^a

^a Reagents: (a) MeNHOMe·HCl, NEt₃, PyBOP, CH₂Cl₂, 92%; (b) DIBALH, THF, 89%; (c) (i) TMS-I, CH₂Cl₂, (ii) MeOH, CH₂Cl₂, (iii) Fmoc-Cl, Na₂CO₃, H₂O/dioxane, 41%.

amide.²⁶ Thus, commercially available Boc-Glu-O^tBu (**9**) was transformed into amide **10** and reduced with diisobutylaluminum hydride (DIBALH) essentially by following the procedure of Wernic et al.²⁷ for the synthesis of the corresponding L-aspartic acid derivatives. The aldehyde formed in this way spontaneously cyclized to give the 5-hydroxyproline derivative **11** as a pair of diastereoisomers (approximate ratio 1:1). No attempts to separate the diastereoisomers were made. NMR spectra recorded at 20 °C (DMSO-*d*₆) showed each diastereoisomer to exist as a mixture of two rotamers, attributable to the relatively high rotation barrier of the nitrogen-carbon bond of the carbamate function.^{28,29} Variable temperature NMR confirmed the existence of a rotamer mixture. The Boc and *tert*-butyl groups were removed by trimethylsilyl iodide (TMS-I), and the zwitterion formed was directly converted to Fmoc derivative **12**. Also for compound **12**, each diastereoisomer was shown by NMR to exist as a mixture of rotamers.

Scheme 2^a

^a Reagents: (a) paraformaldehyde, TsOH, benzene, 98%; (b) Me₂S·BH₃, THF; (c) PCC, NaHCO₃, Celite, CH₂Cl₂; (d) TsOH, MeOH, 50% from **14**; (e) NaOMe, MeOH, 89%; (f) H₂, Pd/C, EtOH, 83%; (g) (i) KOH(aq), MeOH, (ii) Fmoc-Cl, Na₂CO₃, H₂O/dioxane, 62%.

For the synthesis of the second building block **20**, as is depicted in Scheme 2, a protected uncyclized aldehyde, 2-amino-5-oxopentanoic acid (Aop), is employed as a key intermediate. The nitrogen has to be diprotected in order to avoid the facile cyclization onto the aldehyde function. Thus compound **16**, where Aop is protected as a *N*-(carbobenzyloxy)oxazolidinone,³⁰ was synthesized as described previously.³¹ The formyl group was thereafter protected as the dimethyl acetal, and the resulting compound (**17**) was converted to the free amine **19** via **18**.³² After hydrolysis of the α -methyl ester and subsequent Fmoc protection of the nitrogen, building block **20** was isolated.

The building blocks **12** and **20** were subjected to solid-phase peptide synthesis (SPPS) and incorporated into position 5 of the dimercapto peptide precursors **21** and **22**, respectively (Scheme 3). Upon deprotection and cleavage from the solid phase with TFA, both peptides bicyclized toward the N-terminal end to deliver the Ang II analogues **23a** and **23b**, comprising the 5,9-bicyclic tripeptide units **7a** and **7b**.

Building block **20** was found to give more easily purified bicyclized peptides than building block **12** and was therefore selected for the synthesis of Ang II analogues **24–26** (Scheme 4). The bicyclization delivered one major diastereoisomer except in the case of compounds **24a** and **24b**, where the two ring junction epimers were both isolated. Analogues **24–26** were formed as the predominant components of the reaction mixtures. According to LC–MS analysis none of the major side products (>5% yields as estimated from peak areas) exhibited the same molecular weights as the isolated products, suggesting that the synthesis of **12**

and **20** was accompanied with negligible racemization and that the bicyclizations occur with high regioselectivity. After purification by RP-HPLC, the Ang II analogues **24–26** were isolated in 55–33% yield.

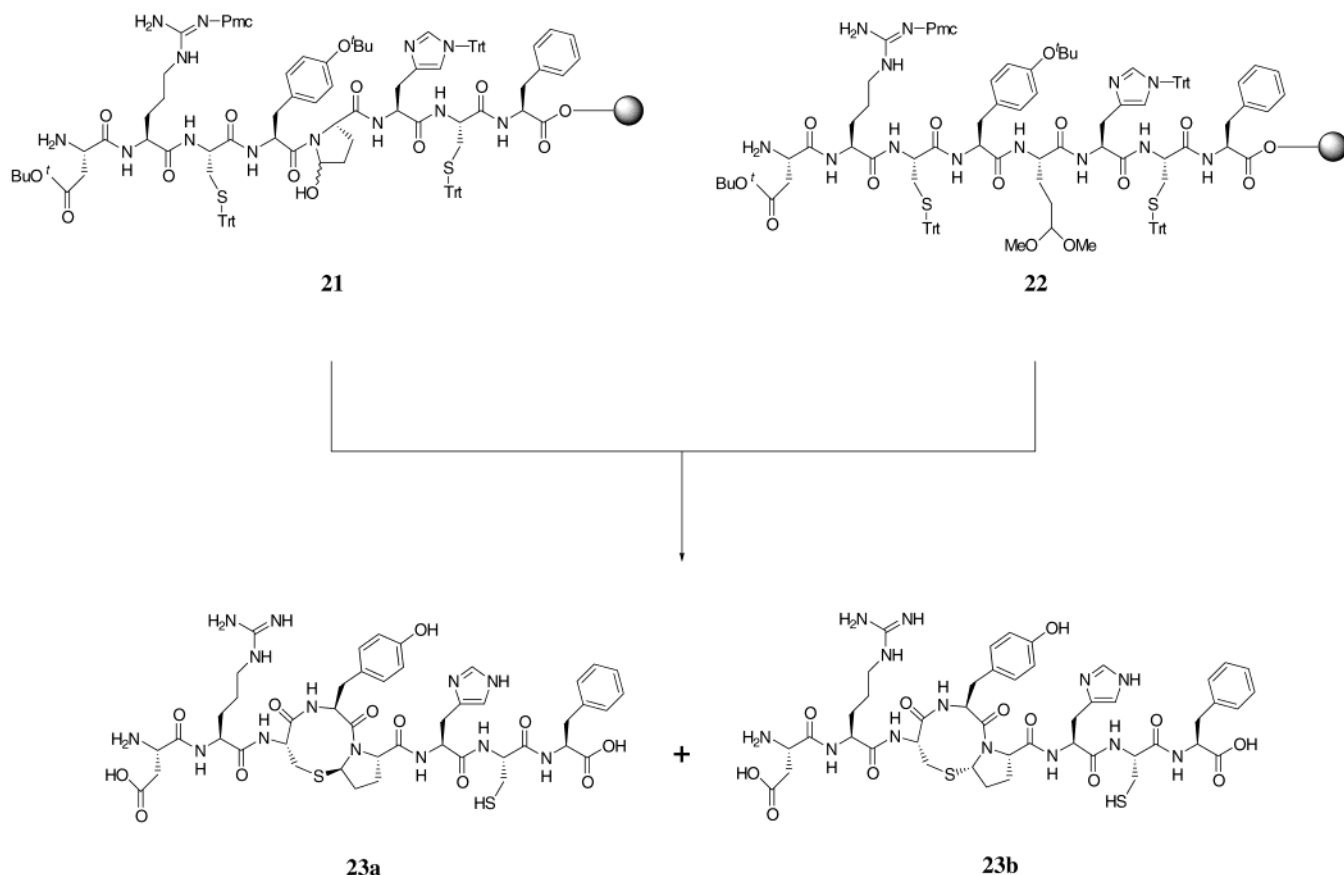
Structural Determination. Proton NMR signals of Ang II analogues **24–26** (Table 1) were assigned from P.E.COSY,³³ TOCSY,³⁴ and ROESY³⁵ spectra, following standard methodology.^{24,36}

Absolute configurations at C- δ of Aop were determined as follows. For **26**, *S* configuration at this center is revealed by NOEs between the proton at Aop- δ and Tyr-NH; the position of the latter with respect to the faces of the bicyclic ring system is determined by its NOE with the proton at Hcy- α . Notably, no NOE is observed between the protons at Aop- δ and Tyr- α . This is in contrast with the observation of a strong NOE between Aop- δ and Tyr- α in **24a**, which is only possible if the configuration at C- δ of Aop is *R*. For compound **25**, the *R* configuration at Aop- δ is established with detection of a NOE between the protons at Aop- δ and His- α . Finally, in **24b**, *S* configuration at C- δ of Aop is indicated, similarly as described for **26**, by a NOE between Aop- δ and Tyr-NH. As before, the position of Tyr-NH was revealed by its NOE with Hcy- α , and the absence of a NOE between Aop- δ and Tyr- α lends additional support to this assignment.

It is notable that the chemical shift for the Aop- δ is correlated to the absolute configuration at this carbon, i.e., higher chemical shifts are observed for the two *S*-configured centers (**24b**: $\delta = 5.34$, **26**: $\delta = 5.52$) than for the *R*-configured centers (**24a**: $\delta = 4.64$, **25**: $\delta = 4.60$). This can be compared to the *R*-configured centers in the previously reported compounds,²⁴ where the chemical shifts ranged between $\delta = 4.79$ and 4.93.

The following observations, which might be related to solution conformations of Ang II analogues **24–26**, were made. For **24a** we note that Tyr-NH has a large coupling constant ($J = 10.3$ Hz) (Table 2), while all other parameters have average values. In **24b**, low chemical shifts are observed for the NH protons of His ($\delta = 7.29$) and Phe ($\delta = 8.02$), and low temperature coefficients (Table 3) are observed for His-NH (0.3) and Cys-NH (2.7). Furthermore, values for the NH coupling constants of Tyr ($J = 4.6$ Hz) and Cys ($J = 6.3$ Hz) are lower than average. Analogue **25** shows unusually high chemical shifts for His protons (δ NH = 9.15, δ H- $\alpha = 5.06$), as well as a large coupling constant between them ($J = 10.2$ Hz). Cys-NH has a low coupling constant ($J = 6.9$ Hz). Temperature coefficients are moderate to high (7.0 for Cys-NH). In **26**, only moderate parameter values are observed. Tyr-NH has a low temperature coefficient of 1.7.

In Vitro Binding Affinity. Compounds **24–26** were screened in a radioligand binding assay based on the displacement of [¹²⁵I]Ang II from rat AT₁ receptors stably expressed by Chinese hamster ovary (CHO) cells.^{37,38} Compounds exhibiting affinity (i.e., compound **26**) were further evaluated in a second radioligand binding assay on AT₁ receptors in rat liver membranes^{11,39} in order to obtain more precise K_i values. Ang II analogue **26** displayed an affinity with a K_i value of 750 nM in this assay. The results from the two receptor binding assays are shown in Table 4. Ang II,

Scheme 3^a

^a Treatment of the dimercapto precursors **21** and **22** with TFA delivered the N-terminal-bicyclized Ang II analogues **23a** and **23b**.

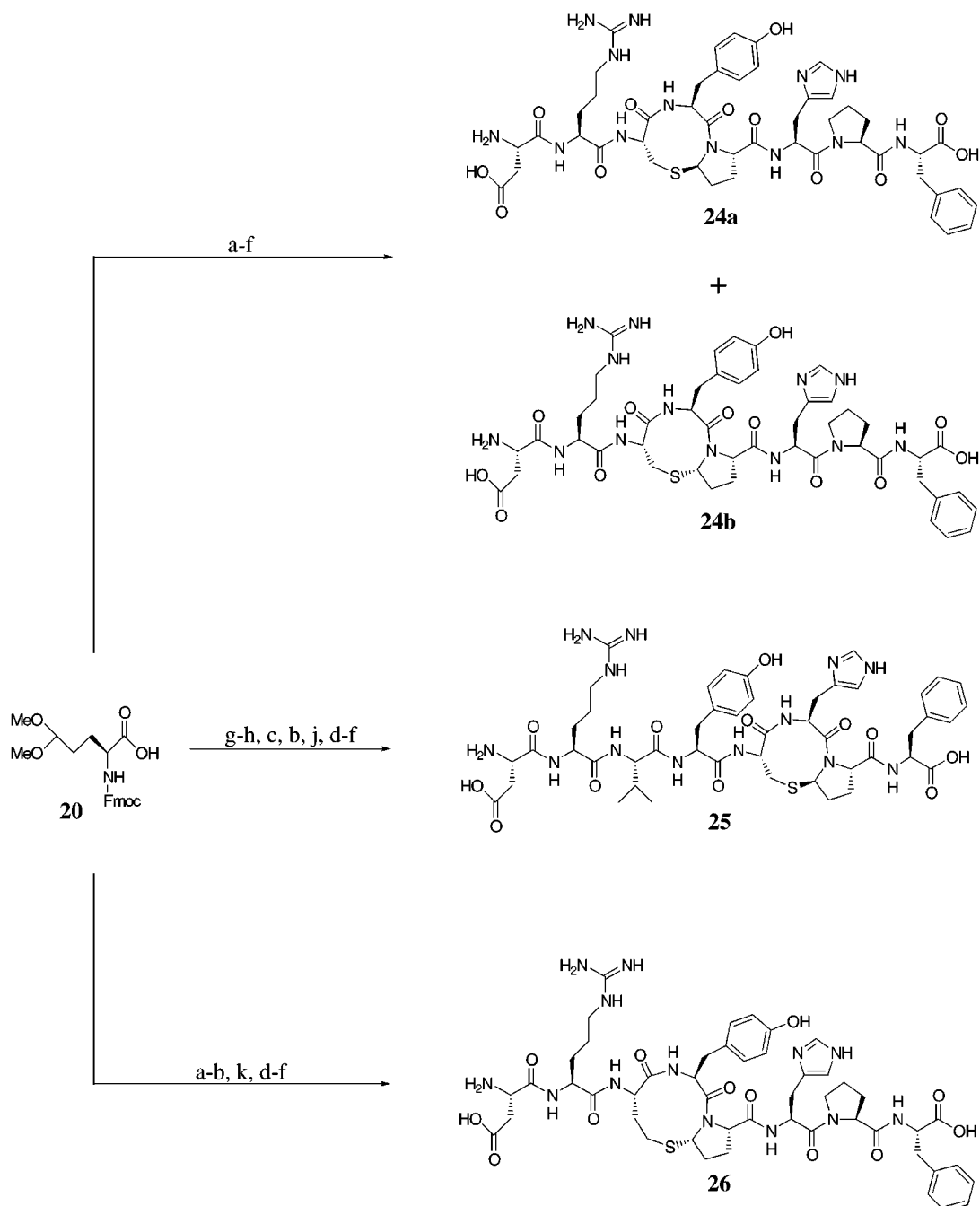
c[Hcy^{3,5}]Ang II, **2**, and the nonpeptide AT₁ antagonist DuP 753 were used as reference substances in both assays.

Theoretical Conformational Characterization of Scaffolds 7a, 7b, and 8. Conformational analysis was performed on the model compounds of scaffolds **7a**, **7b**, **8**, and **27** (See Charts 2 and 3). The conformational properties of the disulfide scaffold **27**, incorporated in the potent Ang II agonist **3** (Chart 1), have been reported previously.^{11,40} We reanalyzed **27** to allow for a direct comparison with the model compounds of our scaffolds (see Discussion). We also included the blocked Ala-Ala-Ala tripeptide **28** in the analyses, as a linear reference peptide. The Amber* force field and the GB/SA water solvation model⁴¹ within Macromodel (version 5.5)⁴² were used in the calculations, and all conformations within 5 kcal/mol of the lowest-energy minimum were characterized. The number of conformations within 5 kcal/mol of the global energy minimum found for model compounds **7a**, **7b**, **8**, **27**, and **28** was 14, 21, 44, 58, and 24, respectively.

To characterize model compounds **7a**, **7b**, and **8**, we studied their β -turn-inducing propensities by measuring the distance between C _{α} of the first residue to C _{α} of the fourth residue. In a β -turn, by definition, this distance should be less than 7 Å and the tetrapeptide sequence making up the β -turn should not be part of an α -helical region.⁴³ For the model compounds used in this study, two locations of the β -turn are available, either between residues 1 and 4 (C _{α 1}–C _{α 4} < 7 Å) or between residues 2 and 5 (C _{α 2}–C _{α 5} < 7 Å, see Figure 1). In the scatter

plot in Figure 2a, these distances are plotted for all conformations within 5 kcal/mol of the lowest-energy conformation. Only **7a** and **28** adopt β -turns as defined by the C _{α 1}–C _{α 4} distance. It should be noted that this turn cannot be stabilized by an intramolecular hydrogen bond in **7a**, since the nitrogen of residue 4 lacks a hydrogen atom. Model compounds **7b** and **8** only adopt β -turns as defined by the C _{α 2}–C _{α 5} distance. Nine out of the 21 conformations of **7b** and 19 out of the 44 conformations of **8** adopt these β -turns. Five of the β -turn conformations of **7b** and six of the β -turn conformations of **8** correspond to the type I β -turn.⁴⁴ In Figure 1, a conformation of **7b** adopting a type I β -turn is shown. Since a proline derivative is present in position 3 in the β -turn between C _{α 2}–C _{α 5}, we also searched for type VI β -turns.^{44,45} However, this turn (type VIa) was only found in one of the conformations of **8**.

The conformational preferences of the backbone torsion angles that are restricted within the bicyclic moiety of **7a**, **7b**, and **8** (Ψ_2 , Φ_3 , Ψ_3 , and Φ_4 ; see Figure 1) were also studied. In Figure 2b the Φ_3 , Ψ_3 plot and in Figure 2c the Φ_4 , Ψ_2 plot of all conformations within 5 kcal/mol of the lowest-energy conformation are shown. In Figure 2b it can be seen that the stereochemically identical compounds **7b** and **8** have similar torsion angle values. In the region $\Phi_3 = -60^\circ$ and $\Psi_3 = -30^\circ$, the type I β -turns are found for compounds **7b** and **8**. The reference compound **28** only populates this region in conformations above 5 kcal/mol. All conformations of **7a** and the rest of the conformations of **7b** and **8** are found in

Scheme 4^a

^a Reagents: (a) (i) His(Trt)-Pro-Phe-Wang resin, HBTU, NMM, DMF, (ii) piperidine, DMF; (b) (i) Fmoc-Tyr(^tBu), HBTU, NMM, DMF, (ii) piperidine, DMF; (c) (i) Fmoc-Cys(Trt), HBTU, NMM, DMF, (ii) piperidine, DMF; (d) (i) Fmoc-Arg(Pmc), HBTU, NMM, DMF, (ii) piperidine, DMF; (e) (i) Fmoc-Asp(O^tBu), HBTU, NMM, DMF, (ii) piperidine, DMF; (f) TFA/H₂O; (g) (i) Phe-Wang resin, HBTU, NMM, DMF, (ii) piperidine, DMF; (h) (i) Fmoc-His(Trt), HBTU, NMM, DMF, (ii) piperidine, DMF; (j) (i) Fmoc-Val, HBTU, NMM, DMF, (ii) piperidine, DMF; (k) (i) Fmoc-Hcy(Trt), HBTU, NMM, DMF, (ii) piperidine, DMF. Hcy is used as the abbreviation for homocysteine.

the upper left corner of Figure 2b. In the Φ_4, Ψ_2 plot all the model compounds of the bicyclic scaffolds seem to adopt Φ_4 values around -80° and Ψ_2 -values around 150° . As depicted in Figure 2b,c, the linear peptide **28** adopts different backbone torsion angles than **7a**, **7b**, and **8**. It also seems that the conformational space available to each of the bicyclic compounds is reduced as compared to the linear peptide **28**.

Finally, we monitored the effect of bicyclization on the overall geometry of the tripeptidic moieties by analyzing the torsion angles $X_1 = (N2-C_{\alpha}2-C_{\alpha}3-C_{\beta}3)$, $X_2 = (C_{\beta}3-C_{\alpha}3-C_{\alpha}4-C(4)O)$, and $X_3 = (N2-C_{\alpha}2-C_{\alpha}4-C(4)O)$ (Fig-

ure 1). X_1 , X_2 , and X_3 describe the important directions of the incoming backbone, the side chain of R_2 , and the outgoing backbone with respect to each other. When these torsion angles were used to analyze the conformational space available to the model compounds, a slightly different picture emerges (see Figure 3a). Conformations close to each other in this 3D plot should have similar geometries with respect to X_1 , X_2 , and X_3 , but not necessarily with respect to the backbone torsion angles. As illustrated in Figure 3a, the model compound of scaffold **7a** is located in two different conformational regions and therefore seems to have the most well-

Table 1. ¹H NMR Chemical Shifts for Ang II Analogues **24–26** (DMSO-*d*₆ Solution, 400 MHz)

| compd (temp) | residue | NH | H-α | H-β | H-β' | other |
|--------------------|--------------------|------|------|------|------|--|
| 24a (35 °C) | Asp | | 4.10 | 2.80 | 2.67 | |
| | Arg | 8.51 | 4.35 | 1.60 | 1.48 | 7.60 (NHε), 3.07 (Hδ, Hδ'), 1.48 (Hγ, Hγ') |
| | Cys | 8.11 | 4.21 | 2.90 | 2.84 | |
| | Tyr | 9.03 | 4.87 | 3.10 | 2.60 | 6.99 (2H, ortho), 6.59 (2H, meta) |
| | Aop | | 4.23 | 2.14 | 1.63 | 4.64 (Hδ), 2.24, 1.93 (Hγ, Hγ') |
| | His | 8.28 | 4.79 | 3.02 | 2.90 | 8.92 (H2), 7.38 (H4) |
| | Pro | | 4.38 | 2.01 | 1.80 | 3.56, 3.45 (Hδ, Hδ'), 1.80 (Hγ, Hγ') |
| | Phe | 8.19 | 4.44 | 3.03 | 2.94 | 7.27–7.16 (5H, Ar) |
| | 24b (35 °C) | Asp | | 4.12 | 2.80 | 2.68 |
| Arg | | 8.55 | 4.53 | 1.64 | 1.57 | 7.48 (NHε), 3.06 (Hδ, Hδ'), 1.51 (Hγ, Hγ') |
| Cys | | 7.64 | 4.77 | 3.91 | 3.00 | |
| Tyr | | 8.84 | 4.27 | 3.04 | 2.87 | 7.04 (2H, ortho), 6.69 (2H, meta) |
| Aop | | | 4.20 | 2.20 | 1.32 | 5.34 (Hδ), 1.98, 1.89 (Hγ, Hγ') |
| His | | 7.29 | 4.86 | 3.11 | 3.01 | 8.87 (H2), 7.38 (H4) |
| Pro | | | 4.40 | 1.98 | 1.71 | 3.49 (Hδ, Hδ'), 1.79 (Hγ, Hγ') |
| Phe | | 8.02 | 4.43 | 3.08 | 2.92 | 7.27–7.16 (5H, Ar) |
| 25 (25 °C) | | Asp | | 4.11 | 2.79 | 2.63 |
| | Arg | 8.57 | 4.34 | 1.62 | 1.49 | 7.66 (NHε), 3.07 (Hδ, Hδ'), 1.50, 1.45 (Hγ, Hγ') |
| | Val | 7.78 | 4.13 | 1.93 | | 0.74, 0.75 (Hγ) |
| | Tyr | 8.00 | 4.47 | 2.80 | 2.64 | 7.00 (2H, ortho), 6.61 (2H, meta) |
| | Cys | 8.12 | 4.18 | 2.88 | 2.88 | |
| | His | 9.15 | 5.06 | 3.19 | 2.86 | 8.90 (H2), 7.28 (H4) |
| | Aop | | 4.31 | 2.12 | 1.75 | 4.60 (Hδ), 2.26, 1.96 (Hγ, Hγ') |
| | Phe | 8.18 | 4.40 | 3.00 | 2.88 | 7.27–7.16 (5H, Ar) |
| | 26 (25 °C) | Asp | | 4.11 | 2.79 | 2.66 |
| Arg | | 8.56 | 4.35 | 1.65 | 1.49 | 7.65 (NHε), 3.07 (Hδ, Hδ'), 1.49 (Hγ, Hγ') |
| Hcy | | 7.98 | 4.43 | 2.22 | 1.81 | 2.67 (Hγ, Hγ') |
| Tyr | | 8.49 | 4.52 | 2.93 | 2.93 | 7.04 (2H, ortho), 6.66 (2H, meta) |
| Aop | | | 4.20 | 2.06 | 1.89 | 5.52 (Hδ), 2.00, 1.82 (Hγ, Hγ') |
| His | | 8.16 | 4.78 | 3.05 | 2.93 | 8.91 (H2), 7.42 (H4) |
| Pro | | | 4.39 | 2.05 | 1.81 | 3.56, 3.48 (Hδ, Hδ'), 2.81 (Hγ, Hγ') |
| Phe | | 8.28 | 4.44 | 3.03 | 2.94 | 7.27–7.16 (5H, Ar) |

Table 2. *J*_{NH-Cα} Coupling Constants for Ang II Analogues **24–26** (DMSO-*d*₆ Solution, 400 MHz)^a

| compd (temp) | residue | <i>J</i> _{NH-Cα} | compd (temp) | residue | <i>J</i> _{NH-Cα} | compd (temp) | residue | <i>J</i> _{NH-Cα} | compd (temp) | residue | <i>J</i> _{NH-Cα} |
|--------------------|---------|---------------------------|--------------------|---------|---------------------------|-------------------|---------|---------------------------|-------------------|---------|---------------------------|
| 24a (35 °C) | Asp | | 24b (35 °C) | Asp | | 25 (25 °C) | Asp | | 26 (25 °C) | Asp | |
| | Arg | 7.7 | | Arg | 7.5 | | Arg | 7.9 | | Arg | 7.9 |
| | Cys | 7.2 | | Cys | 6.3 | | Val | 8.9 | | Hcy | 7.4 |
| | Tyr | 10.3 | | Tyr | 4.6 | | Tyr | 8.0 | | Tyr | 7.3 |
| | Aop | | | Aop | | | Cys | 6.9 | | Aop | |
| | His | 8.0 | | His | 7.9 | | His | 10.2 | | His | 8.1 |
| | Pro | | | Pro | | | Aop | | | Pro | |
| Phe | 7.7 | Phe | 7.7 | Phe | 8.0 | Phe | 7.8 | | | | |

^a *J* values are given in hertz (Hz).**Table 3.** NMR Temperature Coefficients of NH Chemical Shifts for Compounds **24–26** (DMSO-*d*₆ Solution, 400 MHz)^a

| compd | residue 2 | residue 3 | residue 4 | residue 5 | residue 6 | residue 7 | residue 8 |
|------------|-----------|-----------|-----------|-----------|-----------|-----------|-----------|
| 24a | 2.8 | 5.6 | 4.0 | <i>b</i> | 4.4 | <i>c</i> | 4.8 |
| 24b | 3.7 | 2.7 | 3.7 | <i>b</i> | 0.3 | <i>c</i> | 5.7 |
| 25 | 2.7 | 4.3 | 3.7 | 7.0 | 4.0 | <i>b</i> | 4.7 |
| 26 | 2.6 | 4.3 | 1.7 | <i>b</i> | 5.4 | <i>c</i> | 4.0 |

^a Δδ/Δ*T* (ppb/K). ^b No NH (part of the bicyclic ring system). ^c No NH (proline).

defined geometry of the scaffolds. The model compound **7b** can be found in three different regions, while **8** and especially **28** seem to be more conformationally diverse. There is one region, indicated with a circle, that is common to **7a**, **7b**, and **8** and close also to the reference compound **28**. When the lowest-energy conformation found in the circle for each of these compounds is superimposed, as shown in Figure 3b, the overall topography of these conformations is similar. This analysis based on the X₁–X₃ torsion angles is especially useful for the identification of the scaffold which best mimics the topographic conformational profile of a putative target tripeptide moiety.

Table 4. In Vitro Receptor Binding Affinities

| compd | binding on rat AT ₁ receptors expressed by CHO cells IC ₅₀ (nM) | binding on AT ₁ receptors in rat liver membranes K _i (nM) |
|------------------------------|---|---|
| Ang II | 1.5 | 0.53 |
| c[Hcy ^{3,5}]Ang II | 0.2 | 0.19 |
| DuP 753 | 40 | 15 |
| 24a | > 10 000 | |
| 24b | > 10 000 | |
| 25 | > 10 000 | |
| 26 | 800 | 750 |

Discussion

We have demonstrated previously²⁴ that an Ang II derivative with an aspartic acid-derived aldehyde building block (*n* = 1) in the 5-position and cysteine residues in both positions 3 and 7 afforded regioselective C-terminal-directed bicyclization (Scheme 5). The ready formation of the 5-membered ring in favor of 4-, 7-, or 8-membered rings was assumed to provide the driving force. The one-carbon extension (*n* = 2) also gives the option for bicyclization toward the C-terminal end, but by formation of a 6-membered ring. However, cyclization

Chart 3

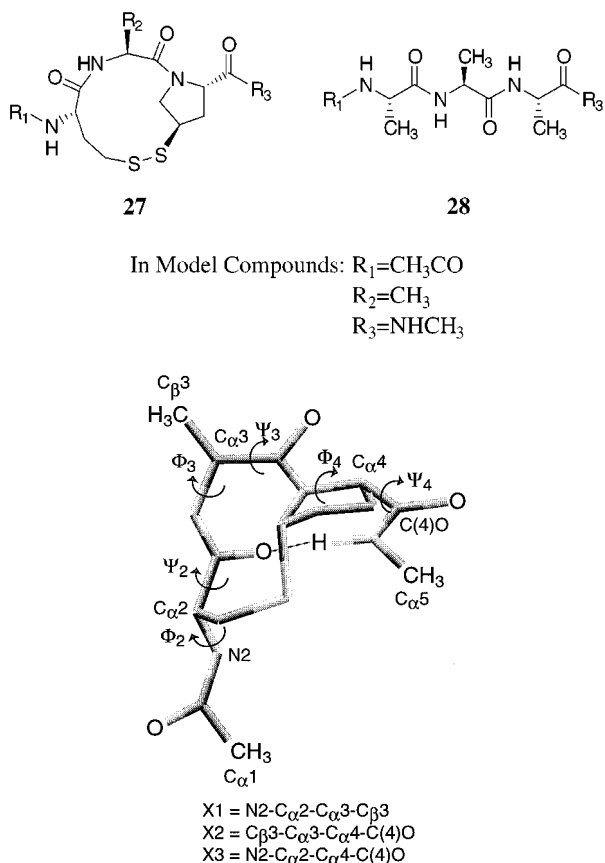


Figure 1. Parameters used to characterize the scaffolds. The conformation of model compound **7b** shown in the figure adopts a type I β -turn. The relative steric energy of this conformation is $\Delta E = 1.0$ kcal/mol.

in the opposite direction, toward the N-terminal end, is now strongly favored, and formation of the 5-membered ring as opposed to the 6-membered ring seems to govern the regioselectivity. Thus, the regioselectivity of the bicyclization can be altered, simply by varying the chain length of the incorporated aldehyde precursor (Scheme 5). While the C-terminal-directed bicyclization ($n = 1$) for the production of rigid tripeptide mimetics proceeds with very high stereoselectivity, both epimers are formed in some cases with N-terminal-directed bicyclizations.

Marshall's and Baldwin's groups have reported two complementary bicyclization methodologies for the preparation of bicyclic dipeptide scaffolds related to ours, but with the inclusion of oxygen in the larger ring. Marshall's procedure^{46–48} relied on an anodic oxidation of a proline residue as a key step. Baldwin⁴⁹ used (*S*)-but-3-enylglycine as aldehyde precursor, reacting with an L-serine hydroxyl group, to form the oxazabicycloalkane system. An elegant example of an aldehyde side chain to N-terminal cyclization, to afford a thiazolidine fused to a large ring, consisting of 10 amino acid residues, has been reported by Tam's group.⁵⁰

In the previous study, we demonstrated that the bicyclic tripeptide scaffolds **5** and **6** preferentially induce β -turn geometries of the nonclassical type.²⁴ In the present study we report that scaffolds **7a**, **7b**, and **8** also can adopt β -turns, of which some correspond to the type I β -turn. When the distribution of backbone torsion

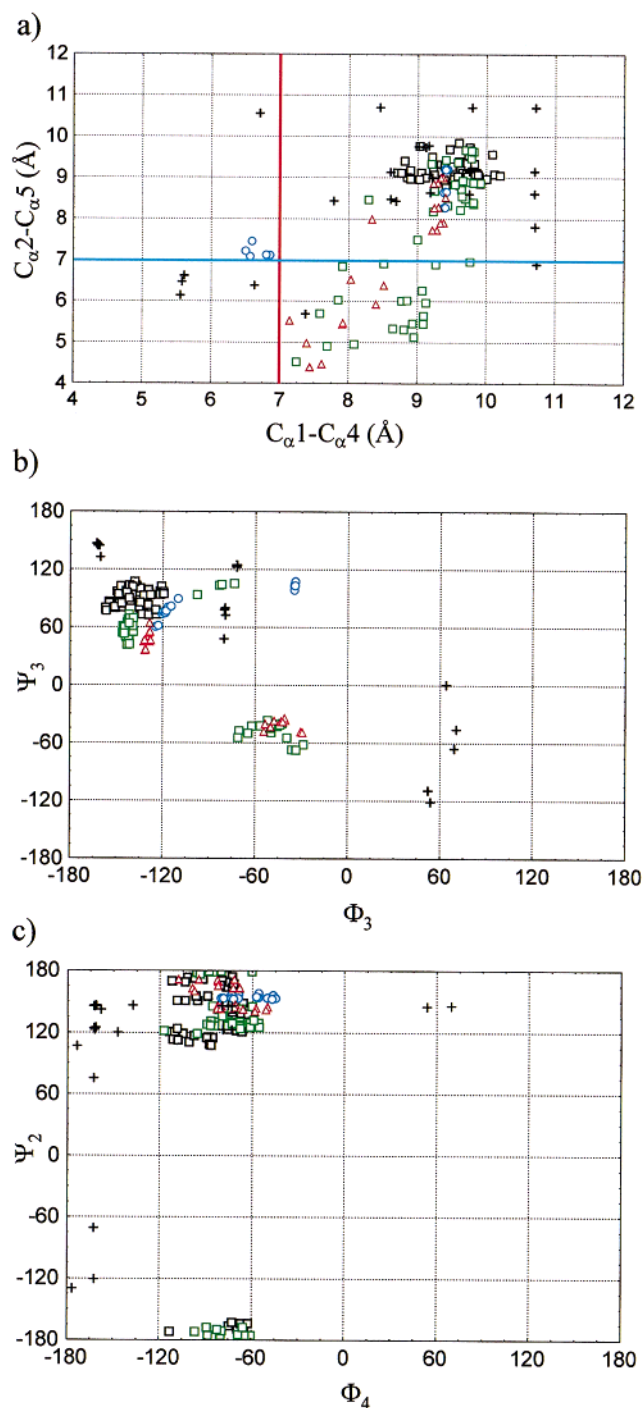
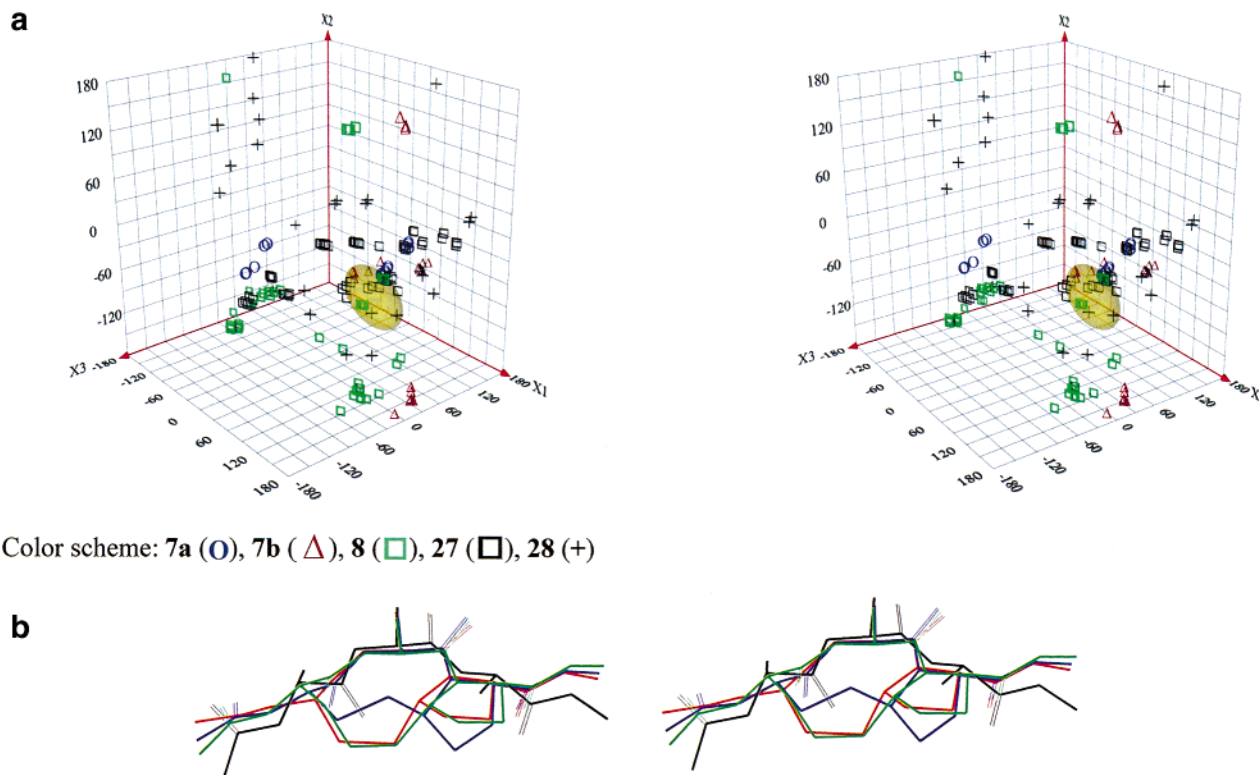


Figure 2. (a) Scatter plot of $\text{C}\alpha 1\text{-C}\alpha 4$ and $\text{C}\alpha 2\text{-C}\alpha 5$ distances for all conformations below 5 kcal/mol of the lowest-energy conformation for model compounds **7a**, **7b**, **8**, **27**, and **28**. Conformations to the left of the red line have $\text{C}\alpha 1\text{-C}\alpha 4$ distances below 7 Å, and conformations below the blue line have $\text{C}\alpha 2\text{-C}\alpha 5$ distances below 7 Å. (b) Scatter plot of backbone torsion angles Φ_3 and Ψ_3 for all conformations below 5 kcal/mol of the lowest-energy conformation for model compounds **7a**, **7b**, **8**, **27**, and **28**. (c) Scatter plot of backbone torsion angles Φ_4 and Ψ_2 for all conformations below 5 kcal/mol of the lowest-energy conformation for **7a**, **7b**, **8**, **27**, and **28**.

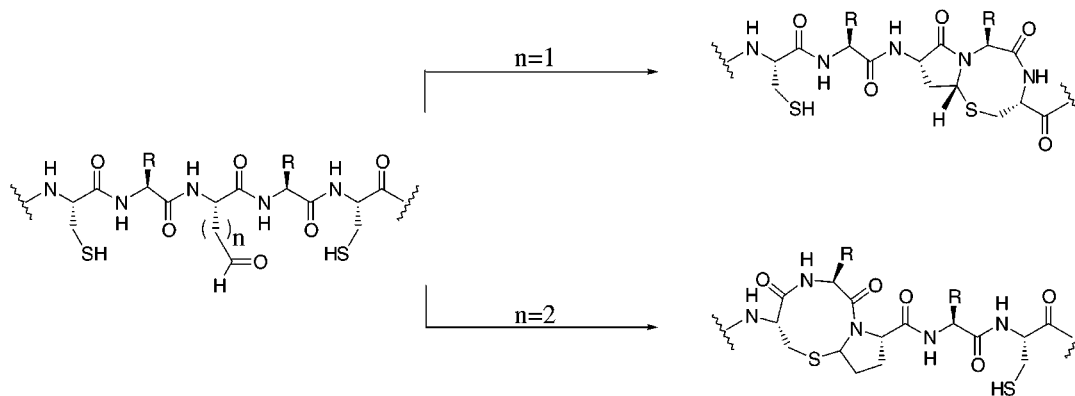
angles are analyzed, a different conformational distribution, as well as a restriction in conformational space, can be seen for the bicyclic model compounds **7a**, **7b**, and **8** as compared to the linear peptide **28**.



Color scheme: **7a** (○), **7b** (△), **8** (□), **27** (◻), **28** (+)

Figure 3. (a) Stereo 3D plot of torsion angles $X_1 = (\text{N}2-\text{C}_{\alpha}2-\text{C}_{\alpha}3-\text{C}_{\beta}3)$, $X_2 = (\text{C}_{\beta}3-\text{C}_{\alpha}3-\text{C}_{\alpha}4-\text{C}(4)\text{O})$, and $X_3 = (\text{N}2-\text{C}_{\alpha}2-\text{C}_{\alpha}4-\text{C}(4)\text{O})$ for all conformations below 5 kcal/mol of the lowest-energy conformation for model compounds **7a**, **7b**, **8**, **27**, and **28**. (b) Stereo image of the rms best fit of the lowest-energy conformations found within the circle indicated in the 3D plot in part a above for each of the model compounds **7a**, **7b**, **8**, and **28**. Color scheme: **7a** (blue) $\Delta E = 0$ kcal/mol, **7b** (red) $\Delta E = 1.2$ kcal/mol, **8** (green) $\Delta E = 1.2$ kcal/mol, and **28** (black) $\Delta E = 2.1$ kcal/mol. N2, $\text{C}_{\alpha}2$, $\text{C}_{\alpha}3$, $\text{C}_{\beta}3$, $\text{C}_{\alpha}4$, and C(4)O were included in the fitting procedure.

Scheme 5^a



^a The regioselectivity of the bicyclization can be altered, simply by varying the chain length of the incorporated aldehyde precursor.

It is generally accepted that in Ang II, Val³, Ile⁵, and Pro⁷ have conformational stabilizing roles.⁵¹ Marshall et al. have demonstrated that bicyclization constraints in the 3–5 and 5–7 regions delivered the high-affinity Ang II analogues **3** and **4**. We were encouraged therefore to incorporate the new aldehyde precursor in both positions 5 and 7, to enforce constraint into these two regions. The receptor binding studies of **24**–**26** showed that Ang II analogue **26**, where the bicyclization had been executed in the 3–5 region, exhibited affinity, although weak ($K_i = 750$ nM), to the AT₁ receptor. The most potent of the Ang II analogues synthesized by Marshall et al., the bicyclic disulfide **3** ($\text{IC}_{50} = 1.3$ nM),¹¹ differs from the most potent in our series (i.e., **26**) with respect to the position of the sulfur atom and the

stereochemistry at the ring junction of the bicyclic system, and also with respect to position 1, where a Sar residue is present in **3**. Such a Sar residue is known to enhance the receptor binding affinity of Ang II analogues 3–10 times^{14,52} and can therefore account for part of the difference in receptor binding affinity between **3** and **26**.

The major reason for the difference in binding affinity between these two octapeptides is more likely due to conformational effects. Conformational studies with NMR have previously supported the presence of multiple conformers for Ang II and Ang II analogues in solution.^{16,53–56} NMR data (DMSO-*d*₆) and independent energy calculations have been presented for Ang II analogue **3**.¹⁶ These NMR data enable a qualitative

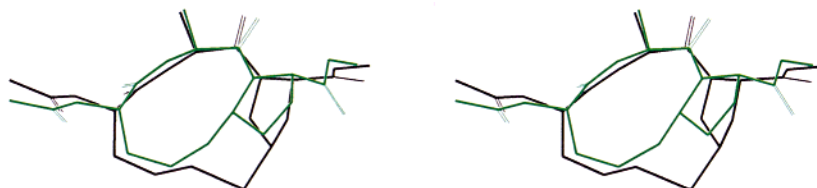


Figure 4. Stereo image of the rms best fit of the lowest energy conformations of **8** (green) and **27** (black). N2, C α 2, C α 3, C β 3, C α 4, and C(4)O were included in the fitting procedure. Mean average distance between fitted atoms = 0.25 Å.

comparison between the conformational profiles of the octapeptides **3** and **26**. This comparison shows that the NH temperature coefficients show essentially the same trend for **26** as compared to **3**, namely that the lowest coefficients are observed for the Arg- and Tyr-NH protons (in **3**:¹⁶ 2.8 and 2.7, in **26**: 2.6 and 1.7). The lower value for the Tyr-NH proton in Ang II analogue **26** could indicate an involvement in an intramolecular hydrogen bond, whereas this is less pronounced in **3**. The NH to C α coupling constants are smaller for **3** than for **26**, except for Tyr where a higher value of 9.3 Hz is observed for octapeptide **3** (cf. $J = 7.3$ Hz for **26**). Taken together, the two octapeptides have similar conformational profiles based on their NMR data.

To compare the conformational preferences of these octapeptides further, we analyzed the Φ and Ψ plots (Figure 2b,c) and the X $_1$ -X $_3$ plot (Figure 3a) obtained for the corresponding tripeptidic model compounds **8** and **27**. In this analysis we assumed that the conformational preferences of the bicyclic scaffolds would not change significantly when they are inserted into Ang II. Thus, if the overall geometry of these scaffolds is similar, octapeptides **3** and **26** should (at least based on conformational reasoning) be able to present the pharmacophore groups in the same 3D arrangement. In fact, conformations with similar torsion angles can be found for **27** and all the other bicyclic model compounds. The overall similarities in topography of model compounds **8** and **27** are shown in Figure 3a and are illustrated further in Figure 4, in which the lowest-energy conformation of **8** and **27** is superimposed. In summary, our conformational analysis of the model compounds does not allow for rationalization of the difference in affinity between Ang II analogues **3** and **26**.

Subtle geometrical variations in the scaffolds apparently affect the affinity, which in turn is largely determined by the relative spatial orientation of side-chain pharmacophores. Thus, access to an armory of simple, complementary synthetic procedures which provides a diversity of scaffolds, including classical secondary structure mimetics, and that allows the full conformational space to be covered is highly desirable in the wait for 3D structural data of peptide/G-protein-coupled receptors.

Conclusion

We have developed an experimentally simple procedure on solid phase for the construction of new tripeptidic 5,9- and 5,10-fused thiazabicycloalkane tripeptide mimetics. This N-terminal-directed bicyclization, relying on masked aldehyde precursors derived from L-glutamic acid as key building blocks, provides a complement to the previously reported related bicyclization using an

aspartic acid-derived precursor to induce cyclization toward the C-terminal end of the peptide. Thus, the regioselectivity of the bicyclization can be reversed, simply through variation of the chain length of the incorporated aldehyde precursor. Insertion of these new bicyclic tripeptide scaffolds into the 3-5- and 5-7-positions of Ang II delivered one analogue (**26**) with an AT $_1$ receptor affinity of $K_i = 750$ nM. This Ang II analogue is structurally very similar to the highly potent bicyclic mercaptoproline derivative **3** (IC $_{50} = 1.3$ nM), suggesting that minor structural alterations have a large impact on the affinity.

Although only a few examples of the application of the presented bicyclization concept are given herein, we believe that the procedure should be amenable to modifications to allow for the introduction of side chains other than Tyr and His in the turn region. The procedure should be applicable also to the elaborations of other target peptides and should hopefully serve as a valuable research tool for the medicinal chemist.

Experimental Section

Chemistry. General Comments. ^1H and ^{13}C NMR spectra were recorded on a JEOL JNM-EX270 at 270 (67.8) MHz, on a JEOL JNM-EX400 at 400 (100.5) MHz, or on a Varian Unity 400 spectrometer at 400 (100.6) MHz. Spectra were recorded at ambient temperature unless otherwise noted. Chemical shifts are reported as δ values (ppm), referenced to Me $_4\text{Si}$. IR spectra were recorded on a Perkin-Elmer model 1605 FT-IR instrument and are reported as ν_{max} (cm $^{-1}$). Optical rotations were measured at ambient temperature on a Perkin-Elmer model 241 polarimeter. Melting points (uncorrected) were determined in open glass capillaries in a melting point microscope. Elemental analyses were performed by Mikro Kemi AB, Uppsala, Sweden. High-resolution mass spectroscopy (HRMS) was performed by Dr. S. Gohil, Department of Chemistry, SLU, Uppsala, Sweden. Flash column chromatography was performed using Merck silica gel 60 (40–63 μm) or Riedel-de Haën silica gel S (32–63 μm). Thin-layer chromatography (TLC) was performed using aluminum sheets pre-coated with silica gel 60 F $_{254}$ (0.2 mm, E. Merck, or 0.25 mm, Macherey-Nagel). Chromatographic spots were visualized by UV and/or spraying with an ethanolic solution of ninhydrin (2%) followed by heating. Mass spectroscopy was carried out on an Applied Biosystems (Uppsala, Sweden) BIOION 20 plasma desorption mass spectrometer. Amino acid analyses and peptide content determinations were performed by Dr. M. Sundquist, Department of Biochemistry, Biomedical Centre, Uppsala, Sweden, on 24-h hydrolyzates with an LKB 4151 alpha plus analyzer, using ninhydrin detection.

Materials. SPPS resins and amino acid derivatives were obtained from Bachem (Bubendorf, Switzerland), Calbiochem-Novabiochem (Läufelfingen, Switzerland), or Alexis Corp. (Läufelfingen, Switzerland). DMF (peptide synthesis grade) was obtained from PerSeptive Biosystems (Hamburg, Germany) and was used without further purification. 2-(1*H*-Benzotriazol-1-yl)-1,1,3,3-tetramethyluronium hexafluorophos-

phate (HBTU) and 1-hydroxybenzotriazole (HOBt) were purchased from Richelieu Biotechnologies (St-Hyacinthe, Qc, Canada). Monoiodinated [¹²⁵I]Ang II (2000 Ci/mmol) was purchased from Euro-Diagnostica AB, Malmö, Sweden, and was prepared by the chloramine-T method.

Solid-Phase Peptide Synthesis (SPPS). The peptides were synthesized on a 60–80- μ mol scale with a Symphony instrument (Protein Technologies Inc., Tucson, AZ) using Fmoc/*tert*-butyl protection. The starting polymer was Fmoc-Phe-Wang resin (0.6 mmol/g), and for the Fmoc amino acids the side chain protecting groups were as follows: Asp(O^tBu), Arg(Pmc), Tyr(^tBu), His(Trt), Cys(Trt), and Hcy(Trt). Removal of the Fmoc group was achieved by reaction with 20% piperidine in DMF for 5 + 10 min. Unless otherwise stated, coupling of the amino acids (125 μ mol) was done in DMF (2.5 mL) using HBTU (125 μ mol) in the presence of NMM (0.5 mmol). Single couplings (60 min) were used for Fmoc-Hcy(Trt) and for compound **20**, double couplings (2 \times 30 min) for the other amino acids. After the introduction of each amino acid, remaining amino groups were capped by addition of 20% acetic anhydride in DMF (1.25 mL) to the coupling mixture and allowing the reaction to proceed for 5 min. No capping was performed in cases where 5-hydroxyproline was present in the resin-bound peptide. After completion of the synthesis, the Fmoc group was removed and the partially protected peptide resin was washed with several portions of DMF and CH₂Cl₂ and dried in a stream of nitrogen and in vacuo. Yields for the purified Ang II analogues were corrected for peptide content.

L-2-(*tert*-Butoxycarbonylamino)-4-(*N*-methoxy-*N*-methylcarbamoyl)butanoic Acid *tert*-Butyl Ester (10**).**⁵⁷ Boc-Glu-O^tBu (**9**) (8.57 g, 28.3 mmol), NEt₃ (4.3 mL, 31 mmol), and PyBOP (16.2 g, 31.1 mmol) were dissolved in CH₂Cl₂ and stirred at room temperature for 10 min. *N,O*-Dimethylhydroxylamine hydrochloride (3.18 g, 32.6 mmol) and a second portion of NEt₃ (4.5 mL, 33 mmol) were added and the mixture was stirred at room temperature for 48 h. The reaction mixture was washed with 10% aqueous citric acid (2 \times 90 mL), saturated aqueous NaHCO₃ (2 \times 150 mL), and brine (1 \times 100 mL). The organic phase was dried (MgSO₄) and evaporated. The residue was purified by flash chromatography (gradient system: pentane/EtOAc 7:3 to pentane/EtOAc 11:9) to give **10** as white crystals (9.06 g, 92%): mp 58–60 °C; TLC *R*_f = 0.45 (pentane/EtOAc 1:1); [α]_D = –18.9° (*c* = 1.0, 99% EtOH); ¹H NMR (CDCl₃) δ 1.43 (s, 9H, C(CH₃)₃), 1.46 (s, 9H, C(CH₃)₃), 1.83–1.98 (m, 1H, CH₂), 2.06–2.22 (m, 1H, CH₂), 2.39–2.62 (m, 2H, CH₂), 3.17 (s, 3H, NCH₃), 3.67 (s, 3H, OCH₃), 4.19 (m, 1H, 2), 5.18 (br d, *J* = 7.6 Hz, 1H, NH); ¹³C NMR (CDCl₃) δ 27.4 (CH₂), 27.8 (C(CH₃)₃), 27.9 (CH₂), 28.2 (C(CH₃)₃), 32.1 (NCH₃), 53.6 (2), 61.1 (OCH₃), 79.4, 81.7 (C(CH₃)₃), 155.4 (CO Boc), 171.4, 173.4 (CO ester and CO carbamoyl); IR (KBr) 3267, 1732, 1708, 1639. Anal. (C₁₆H₃₀N₂O₆) C, H, N.

***N*-(*tert*-Butoxycarbonyl)-5-hydroxy-L-proline *tert*-Butyl Ester (**11**).**^{25,58} Amide **10** (5.00 g, 14.4 mmol) was dissolved in dry THF, under N₂ atmosphere, and cooled to –78 °C. DIBALH (1 M in hexane) (21.7 mL, 21.7 mmol) was added dropwise during 15 min, whereafter the reaction mixture was stirred at –78 °C for 1.5 h. The reaction mixture was partitioned between ether (135 mL) and 10% aqueous citric acid (75 mL). The aqueous phase was further extracted with ether (100 mL). The combined organic layers were washed with 10% aqueous citric acid (1 \times 65 mL) and brine (1 \times 65 mL), dried (MgSO₄), and evaporated. Purification by flash chromatography (gradient system: pentane/EtOAc 9:1 to pentane/EtOAc 3:2) afforded the pure product **11** (3.70 g, 89%), colorless oil, as a pair of diastereoisomers (approximate ratio 1:1). Some peaks in the NMR spectra are duplicated, due to hindered rotation of the carbamate function:^{28,29} TLC *R*_f = 0.45 (pentane/EtOAc 7:3); [α]_D = –62.8° (*c* = 1.0, 99% EtOH); ¹H NMR (DMSO-*d*₆, 90 °C) δ 1.34–1.54 (m, 18H, (C(CH₃)₃)), 1.60–2.45 (m, 4H, 3 and 4), 3.98–4.10 (m, 1H, 2), 4.93 and 5.27 (2 br s, 1H together, exchangeable with D₂O, OH), 5.33–5.44 (m, 1H, 5); ¹³C NMR (DMSO-*d*₆, 90 °C) δ 27.0 (3), 27.4, 27.5, 27.8

(C(CH₃)₃, 31.7, 32.8 (4), 59.2, 59.6 (2), 78.8, 79.7, 80.0 (C(CH₃)₃), 80.6, 81.2 (5), 152.7 (CO Boc), 171.0 (CO carboxylic acid); IR (neat) 3454, 1741, 1703. Anal. (C₁₄H₂₅NO₅) C, H, N.

***N*-(9-Fluorenylmethoxycarbonyl)-5-hydroxy-L-proline (**12**).** The proline derivative **11** (0.42 g, 1.5 mmol) was dissolved in CH₂Cl₂ under N₂ atmosphere at room temperature. TMS-I (0.70 mL, 4.9 mmol) was added and the mixture was stirred at room temperature. After 50 min the reaction was quenched with MeOH (3.6 mL, 89 mmol) and stirred for another 20 min. The reaction mixture was evaporated and the yellow residue was redissolved in a mixture of 10% aqueous Na₂CO₃ (30 mL) and dioxane (15 mL) and cooled to 0 °C. Fmoc-Cl (0.57 g, 2.2 mmol) was dissolved in dioxane (15 mL) and added dropwise, whereafter the reaction was allowed to reach room temperature. The pH was kept around 10–11. After the mixture was stirred at room temperature for 96 h, 10% aqueous citric acid was added to pH 8, and the reaction mixture was washed with ether until TLC showed the water phase to be free from impurities having *R*_f values higher than those of the product (4 \times 100 mL). Ether (200 mL) was added to the water phase, which was then acidified to pH 2–3 with 10% aqueous citric acid, under vigorous stirring. The phases were separated and the water phase was further extracted with ether (3 \times 150 mL). The combined organic layers were washed with water (2 \times 100 mL), dried (MgSO₄), and concentrated to yield the building block **12** (0.21 g, 41%) as a white foam. NMR spectra show the existence of each diastereoisomer as a pair of rotamers: TLC *R*_f = 0.20 and 0.30 for the two diastereoisomers, respectively (CH₂Cl₂/MeOH 9:1); [α]_D = –43.1° (*c* = 1.0, 99% EtOH); ¹H NMR (CDCl₃, 20 °C) δ 1.70–2.61 (m, 4H, 3 and 4), 4.08–4.78 (m, 5H, OH, 2, CH Fmoc and CH₂ Fmoc), 5.04 (br d), 5.27 (br s) and 5.64 (br d) (1H together, 5), 7.23–7.82 (m, 8H, CH Ar Fmoc); ¹³C NMR (CDCl₃, 20 °C) δ 26.5, 26.9, 28.0, 30.2, 30.9, 31.6, 32.0, 33.2 (3 and 4), 46.8, 47.0 (CH Fmoc), 58.6, 58.8 (2), 66.9, 67.0, 67.9 (CH₂ Fmoc), 81.6, 82.2, 82.3, 82.9 (5), 119.9, 120.0, 120.1, 124.5, 124.7, 124.8, 124.9, 127.0, 127.3, 127.7, 127.8, 127.9 (CH Ar Fmoc), 140.0, 141.11, 141.14, 141.2, 143.30, 143.35, 143.5, 143.6 (C ipso Ar Fmoc), 154.2, 154.8 (CO Fmoc), 176.0, 176.7 (CO carboxylic acid); IR (KBr) 3430, 1704. Anal. (C₂₀H₁₉NO₅·1.25H₂O) C, N; H: calcd, 5.76; found, 5.1. HRMS (FAB) calcd for C₂₀H₁₉NO₅ (M + H⁺): 354.1342. Found: 354.1351.

L-3-(Benzyloxycarbonyl)-4-(3,3-dimethoxypropyl)-1,3-oxazolidin-5-one (17**).**³² L-3-(3-(Benzyloxycarbonyl)-5-oxo-1,3-oxazolidin-4-yl)propanoic acid (**14**) (26.4 g, 90.0 mmol) was converted to L-3-(3-(benzyloxycarbonyl)-5-oxo-1,3-oxazolidin-4-yl)propanal (**16**)^{59–61} as described in the literature.³¹ Crude **16** (18.9 g) and *p*-toluenesulfonic acid (monohydrate, 98.5%) (0.65 g, 3.4 mmol) were dissolved in MeOH (1 L). After stirring at room temperature for 2 h, most of the solvent was evaporated and the residue was partitioned between EtOAc (300 mL) and saturated aqueous NaHCO₃ (100 mL). The organic phase was washed with brine (100 mL), dried (MgSO₄), and concentrated. Purification by flash chromatography (gradient system: pentane/EtOAc 4:1 to pentane/EtOAc 2:1) gave the product **17** as a colorless oil (14.5 g, 50% over three steps, from compound **14**): TLC *R*_f = 0.65 (pentane/EtOAc 3:2); [α]_D = +82.2° (*c* = 1.0, CHCl₃); ¹H NMR (CDCl₃) δ 1.59–1.78 (m, 2H, CH₂), 1.86–2.24 (m, 2H, CH₂), 3.27 (s, 6H, CH(OCH₃)₂), 4.28–4.38 (br m, 2H, 3 and 4), 5.12–5.26 (m, 3H, OCH₂N and OCH₂Ar), 5.52 (br s, 1H, OCH₂N), 7.35–7.39 (m, 5H, CH Ar); ¹³C NMR (CDCl₃) δ 25.4, 27.0 (CH₂CH₂), 52.5, 52.6 (CH(OCH₃)₂), 54.2 (4), 67.6 (OCH₂Ar), 77.6 (OCH₂N), 103.5 (3), 128.0, 128.3, 128.4 (CH Ar), 135.2 (ipso Ar), 152.6 (CO Cbz), 171.9 (5); IR (neat) 1803, 1719. Anal. (C₁₆H₂₁NO₆) C, H, N.

L-2-(Benzyloxycarbonylamino)-5,5-dimethoxypentanoic Acid Methyl Ester (18**).**³² Dimethyl acetal **17** (12.0 g, 37.2 mmol) was dissolved in MeOH (500 mL) under N₂ atmosphere and cooled to –12 °C. Sodium methoxide (2.00 g, 37.0 mmol) was suspended in MeOH (45 mL) and added dropwise during 1 h. After stirring for 2 h, aqueous citric acid was added to pH 7–8, and half the amount of solvent was evaporated. The residue was poured into EtOAc (500 mL) and washed with 10%

aqueous NaCl (2 × 500 mL). The organic layer was dried (MgSO₄) and concentrated and the residue was purified by flash chromatography (gradient system: pentane/EtOAc 5:1 to pentane/EtOAc 3:2) to yield **18** (10.7 g, 89%) as a colorless oil: TLC R_f = 0.60 (pentane/EtOAc 3:2); $[\alpha]_D^{25}$ = +7.5° (c = 1.0, CHCl₃); ¹H NMR (CDCl₃) δ 1.56–1.80 (m, 3H, 3_a, 4), 1.85–1.98 (m, 1H, 3_b), 3.29 (s, 3H, CHOC₂H₅), 3.30 (s, 3H, CHOC₂H₅), 3.74 (s, 3H, COOCH₃), 4.34 (app t, 1H, 5), 4.39 (app dd, 1H, 2), 5.11 (s, 2H, OCH₂Ar), 5.38 (br d, J = 7.8 Hz, 1H, NH), 7.29–7.39 (m, 5H, CH Ar); ¹³C NMR (CDCl₃) δ 27.3, 28.2 (3, 4), 52.2 (COOCH₃), 52.8 (CH(OCH₃)₂), 53.4 (2), 66.8 (OCH₂Ar), 103.7 (5), 127.9, 128.0, 128.4 (CH Ar), 136.1 (ipso Ar), 155.8 (CO Cz), 172.6 (1); IR (neat) 3330, 1721. Anal. (C₁₆H₂₃NO₆) C, H, N.

L-2-Amino-5,5-dimethoxypentanoic Acid Methyl Ester (19).^{32,62} Compound **18** (10.5 g, 32.2 mmol) and 10% Pd/C (1.74 g, 1.64 mmol) were mixed in absolute ethanol and stirred under H₂ (1 atm) at room temperature for 2 h. The mixture was filtered through Celite and concentrated. The residue was purified by flash chromatography (gradient system: CH₂Cl₂ to CH₂Cl₂/MeOH 24:1) to give the product **19** (5.08 g, 83%) as a colorless oil: TLC R_f = 0.40 (CH₂Cl₂/MeOH 9:1); $[\alpha]_D^{25}$ = +16° (c = 1.0, CHCl₃); ¹H NMR (CDCl₃) δ 1.47–1.86 (m, 6H, 3, 4 and NH₂), 3.30 (s, 3H, CHOC₂H₅), 3.31 (s, 3H, CHOC₂H₅), 3.44 (dd, J = 5.2, 7.4 Hz, 1H, 2), 3.71 (s, 3H, COOCH₃), 4.36 (t, J = 5.3 Hz, 1H, 5); ¹³C NMR (CDCl₃) δ 28.5 (4), 29.7 (3), 51.8 (COOCH₃), 52.6, 52.7 (CH(OCH₃)₂), 54.0 (2), 104.0 (5), 176.2 (1); IR (neat) 3376, 1737. Anal. (C₈H₁₇NO₄) C, H, N.

L-2-((9-Fluorenylmethyloxycarbonyl)amino)-5,5-dimethoxypentanoic Acid (20).⁶³ To compound **19** (0.48 g, 2.5 mmol) dissolved in MeOH (30 mL) was added 1 M aqueous KOH (2.5 mL, 2.5 mmol) and the mixture was stirred at room temperature for 3.5 h; 10% aqueous citric acid was added to pH 7–8 and the reaction mixture was concentrated to give a solid residue. This solid residue was dissolved in a mixture of 10% aqueous Na₂CO₃ (45 mL) and dioxane (23 mL) and cooled to 0 °C. Fmoc-Cl (0.97 g, 3.7 mmol) dissolved in dioxane (23 mL) was added dropwise, whereafter the reaction was allowed to reach room temperature. The pH was kept around 10–11. Stirring at room temperature was continued for 96 h. The workup was performed through extensive extractions following essentially the same procedure as described for compound **12** to afford pure product **20** as a white foam (0.62 g, 62%): TLC R_f = 0.45 (CH₂Cl₂/MeOH 9:1); $[\alpha]_D^{25}$ = +8.6° (c = 1.0, CHCl₃); ¹H NMR (acetone-*d*₆) δ 1.65–1.81 (m, 3H, 3_a and 4), 1.86–1.97 (m, 1H, 3_b), 3.27 (s, 3H, CHOC₂H₅), 3.28 (s, 3H, CHOC₂H₅), 4.22–4.31 (m, 4H, CH Fmoc, 2 and CH₂ Fmoc), 4.41 (app t, 1H, 5), 6.85 (br d, J = 8.0 Hz, 1H, NH), 7.32 (t, J = 7.6 Hz, 2H, CH Ar Fmoc), 7.41 (t, J = 7.6 Hz, 2H, CH Ar Fmoc), 7.72 (app t, J = 6.9 Hz, 2H, CH Ar Fmoc), 7.85 (d, J = 8.7 Hz, 2H, CH Ar Fmoc); ¹³C NMR (acetone-*d*₆) δ 27.5, 29.5 (3, 4), 47.9 (CH Fmoc), 52.8, 53.0 (CH(OCH₃)₂), 54.4 (2), 67.1 (CH₂ Fmoc), 104.7 (5), 120.7, 126.0, 126.1, 127.8, 128.4 (CH Ar Fmoc), 141.9, 144.8, 145.0 (ipso Fmoc), 157.0 (CO Fmoc), 173.9 (1); IR (KBr) 3324, 1720. Anal. (C₂₂H₂₅NO₆·H₂O) C, H, N.

Ang II Analogues 23a and 23b. Method 1, using Fmoc-5-hydroxy-L-proline (12). Fmoc-Phe-Wang resin (105 mg, 63 μmol) was reacted with the appropriate amino acids as described above (general procedure). However, the hydroxyproline derivative **12** (125 μmol) was coupled for 19.5 h using PyBOP (125 μmol) in the presence of HOBT (125 μmol) and diisopropylethylamine (DIEA) (313 μmol). The next residue, Fmoc-Tyr(O^tBu)-OH, was coupled for 4 h in the same way but using 5 equiv of amino acid, PyBOP, HOBT, and 10 equiv of DIEA. The yield of the partially protected peptide resin was 212 mg (95.6% according to weight increase). The resin was treated with 95% aqueous TFA (2.5 mL) for 2 h and the mixture was then filtered through a small plug of glass wool in a Pasteur pipet. After washing with TFA (3 × 0.3 mL), the combined filtrates were evaporated in a stream of dry nitrogen to ca. 1.5 mL and the product was precipitated by the addition of cold, anhydrous ether (12 mL). The precipitate was collected by centrifugation, washed with ether (4 × 7 mL), and dried. Plasma desorption mass spectrometry (PDMS) analysis revealed that a substantial part of the crude material was still

monotritylated. Therefore, the product was dissolved in TFA (0.75 mL) and a 5% solution of triethylsilane (0.75 mL) was added to produce a nearly colorless solution. Precipitation and washing with ether as described above furnished 44.3 mg (67.7%) of the crude bicyclic Ang II analogue **23**. The peptide (39.4 mg) was dissolved in 0.1% aqueous TFA and purified in three runs by RP-HPLC on a Vydac 10-μm C18 column (1.0 × 25 cm) with an 80-min gradient of 10–50% MeCN in 0.1% aqueous TFA at a flow rate of 3 mL/min. The separation was monitored at 230 nm and by PDMS. Two compounds of the expected mass were isolated. **23a**: 2.9 mg (5.1%); PDMS (MW 1038.0) 1038.7 (M + H⁺). **23b**: 2.2 mg (3.8%); PDMS 1039.0 (M + H⁺).

Method 2, using Fmoc-L-2-amino-5,5-dimethoxypentanoic acid (20). The peptide was synthesized according to the same procedure as in method 1, using PyBOP/HOBT/DIEA for the incorporation of amino acid derivative **20** and for the tyrosine residue. The partially protected peptide resin, 215 mg (95.0%), was cleaved as described above to yield 51.7 mg (79.4%) of crude detritylated product. This material was dissolved in 0.1% aqueous TFA (12 mL) and purified by two runs on a Vydac 10-μm C18 column (2.2 × 25 cm) using an 80-min gradient of 0–40% MeCN in 0.1% aqueous TFA at a flow rate of 4 mL/min. Again, two compounds of the expected mass were obtained. **23a**: 5.7 mg (5.7%); PDMS (MW 1038.0) 1039.0 (M + H⁺); amino acid analysis Asp, 0.99; Arg, 0.99; Tyr, 0.99; His, 1.01; Phe, 1.01; Cys, not determined (nd) (66% peptide); ¹H NMR (DMSO-*d*₆, 25 °C, 400 MHz) δ 1.44 (m, 2H, H γ -Arg, H γ' -Arg), 1.49 (m, 1H, H β -Arg), 1.59 (m, 1H, H β' -Arg), 1.74 (m, 1H, H β -Aop), 1.93 (m, 1H, H γ -Aop), 2.11 (m, 1H, H β' -Aop), 2.22 (m, 1H, H β -Cys⁷), 2.60 (m, 1H, H β -Tyr), 2.68 (m, 1H, H β -Asp), 2.70 (m, 1H, H β' -Cys⁷), 2.77 (m, 1H, H β' -Asp), 2.77 (m, 1H, H γ' -Aop), 2.90 (m, 2H, H β -Cys³, H β' -Cys³), 2.90 (m, 1H, H β -Phe), 2.95 (m, 1H, H β -His), 3.04 (m, 1H, H β' -Phe), 3.06 (m, 2H, H δ -Arg, H δ' -Arg), 3.07 (m, 1H, H β' -His), 3.15 (m, 1H, H β' -Tyr), 4.10 (m, 1H, H α -Asp), 4.21 (m, 1H, H α -Cys³), 4.25 (dm, J = 9.5 Hz, 1H, H α -Aop), 4.34 (m, 1H, H α -Arg), 4.41 (m, 1H, H α -Cys⁷), 4.43 (m, 1H, H α -Phe), 4.52 (ddd, J = 8.4, 7.9, 5.6 Hz, 1H, H α -His), 4.63 (dd, J = 4.8, 1.8 Hz, 1H, H δ -Aop), 4.84 (ddd, J = 10.2, 9.6, 4.7 Hz, 1H, H α -Tyr), 6.57 (m, 2H, meta-Tyr), 7.00 (m, 2H, ortho-Tyr), 7.17–7.26 (m, 5H, Phe), 7.32 (br s, 1H, H δ -His), 7.57 (m, 1H, NH ϵ -Arg), 7.76 (d, J = 7.9 Hz, 1H, NH-Cys⁷), 8.18 (d, J = 7.1 Hz, 1H, NH-Cys³), 8.38 (d, J = 7.8 Hz, 1H, NH-Phe), 8.43 (d, J = 8.4 Hz, 1H, NH-His), 8.54 (d, J = 7.6 Hz, 1H, NH-Arg), 8.90 (br s, 1H, H δ -His), 9.09 (d, J = 10.2 Hz, 1H, NH-Tyr). **23b**: 9.0 mg (10.4%); PDMS 1039.8 (M + H⁺); amino acid analysis Asp, 1.00; Arg, 1.00; Tyr, 0.99; His, 1.01; Phe, 1.00; Cys, nd (75% peptide); ¹H NMR (DMSO-*d*₆, 25 °C, 400 MHz) δ 1.26 (m, 1H, H β -Aop), 1.48 (m, 1H, H β -Arg), 1.48 (m, 2H, H γ -Arg, H γ' -Arg), 1.63 (m, 1H, H β' -Arg), 1.90 (m, 1H, H γ -Aop), 1.97 (m, 1H, H γ' -Aop), 2.18 (m, 1H, H β' -Aop), 2.48 (m, 1H, H β -Cys⁷), 2.65 (m, 1H, H β -Asp), 2.72 (m, 1H, H β' -Cys⁷), 2.76 (m, 1H, H β' -Asp), 2.90 (m, 1H, H β -Tyr), 2.90 (m, 1H, H β -Phe), 2.96 (m, 1H, H β -Cys³), 2.96 (m, 1H, H β -His), 3.00 (m, 1H, H β' -Phe), 3.03 (m, 2H, H δ -Arg, H δ' -Arg), 3.06 (m, 1H, H β' -Tyr), 3.35 (m, 1H, H β' -His), 3.93 (m, 1H, H β' -Cys³), 4.10 (m, 1H, H α -Asp), 4.21 (dd, J = 10.2, 8.5 Hz, 1H, H α -Aop), 4.39 (m, 1H, H α -Cys⁷), 4.41 (m, 1H, H α -Arg), 4.41 (m, 1H, H α -Phe), 4.43 (m, 1H, H α -Tyr), 4.67 (ddd, J = 10.2, 8.6, 4.5 Hz, 1H, H α -His), 4.81 (ddm, J = 6.6, 4.6 Hz, 1H, H α -Cys³), 5.30 (dd, J = 5.7, 1.8 Hz, 1H, H δ -Aop), 6.69 (m, 2H, meta-Tyr), 7.07 (m, 2H, ortho-Tyr), 7.17–7.25 (m, 5H, Phe), 7.44 (m, 1H, NH-His), 7.44 (m, 1H, H δ -His), 7.46 (m, 1H, NH-Cys⁷), 7.65 (m, 1H, NH ϵ -Arg), 8.13 (d, J = 7.7 Hz, 1H, NH-Phe), 8.36 (br, 1H, NH-Cys³), 8.59 (d, J = 7.6 Hz, 1H, NH-Arg), 8.85 (br, 1H, H δ -His), 8.89 (d, J = 3.7 Hz, 1H, NH-Tyr).

Ang II Analogues 24a and 24b. Automated synthesis on an 80-μmol scale according to the general procedure and using **20** for incorporation of the Aop residue provided 245 mg (97.4%) of partially protected resin which was cleaved and deprotected with 95% aqueous TFA (2.5 mL) for 1.5 h. The resin was filtered off and washed with 5% triethylsilane in TFA (3 × 0.3 mL). The peptide was precipitated with cold ether

(10 mL), collected by centrifugation, washed with ether (4 × 7 mL), and dried to yield 71.2 mg (90.5%). The crude material was divided in four aliquots, each dissolved in 0.1% aqueous TFA, containing 15% MeCN (5 mL) and chromatographed on a Vydac 10- μ m C18 column (1 × 25 cm) using a 60-min gradient of 15–45% MeCN in 0.1% aqueous TFA at a flow rate of 3 mL/min. The fractions corresponding to the two major peaks both contained material of the expected mass. **24a**: 19.2 mg (17.0%); PDMS (MW 1032.1); 1033.5 (M + H⁺); amino acid analysis Asp, 1.01; Arg, 0.98; Tyr, 0.99; His, 0.99; Pro, 1.01; Phe, 1.02; Cys, nd (73% peptide). **24b**: 28.1 mg (26.6%); PDMS 1033.7 (M + H⁺); amino acid analysis Asp, 1.01; Arg, 1.02; Tyr, 0.97; His, 0.98; Pro, 1.02; Phe, 1.00; Cys, nd (78% peptide).

Ang II Analogue 25. The partially protected peptide resin prepared by the procedure used for **24** was recovered in 98.4% yield according to the weight increase. Part of the resin (126 mg, 38.8 μ mol) was treated with 95% aqueous TFA and the product was worked up as described for **24**. Yield: 40.1 mg (100%). The product was purified in two runs on a Vydac 10- μ m C18 column (1 × 25 cm) using an 80-min gradient of 10–50% MeCN in 0.1% aqueous TFA at a flow rate of 3 mL/min to yield 24.9 mg (33.0%) of pure **25**: PDMS (MW 1034.0) 1035.1 (M + H⁺); amino acid analysis Asp, 0.98; Arg, 1.01; Val, 0.98; Tyr, 1.13; His, 1.02; Phe, 0.28; Cys, nd (54% peptide).

Ang II Analogue 26. Synthesis, cleavage, and purification were carried out as described for **24** above. The yield of peptide resin was 242 mg (97.2%) and of crude product 59.3 mg (75.6%). The purified material weighed 18.6 mg (15.6%): PDMS (MW 1046.1) 1046.7 (M + H⁺); amino acid analysis Asp, 0.99; Arg, 1.01; Tyr, 0.91; His, 1.00; Pro, 1.00; Phe, 1.10 (overlapping with an impurity derived from Hcy); Hcy, nd (66% peptide).

AT₁ Receptor Binding Assay on CHO Cells. CHO cells stably expressing the rat AT₁ receptor³⁸ were grown in RPMI 1640 medium with L-glutamine, supplemented with 10% fetal calf serum and antibiotic/antimycotic solution, in a humidified atmosphere of 5% CO₂ and 95% air. At 80% confluency, the cells were detached from the flasks by incubation in Hanks' balanced salt solution (HBSS) with 5 mM EDTA, collected by centrifugation, and suspended in binding buffer consisting of minimum essential medium with Earle's salts, 25 mM HEPES, GlutaMax I, 0.2% BSA, 0.02% phenanthroline, leupeptin (0.5 μ g/mL), and bacitracin (0.2 mg/mL). The cells were distributed in a 96-well plate so that each well contained about 50 000 cells. The cells were incubated with a fixed concentration of [¹²⁵I]Ang II (ca. 50 000 cpm, ca. 0.2 nM) and variable concentrations of competing substance, in binding buffer at room temperature, for 1.5 h in a final volume of 50 μ L. After centrifugation, the binding buffer was carefully sucked away and the cells were washed with cold binding buffer and treated with 0.1 M NaOH at 37 °C for 30 min. The mixture was transferred to tubes, and the radioactivity was measured in a gamma counter. Nonspecific binding was determined in the presence of 1 μ M Ang II. All experiments were performed in duplicates. IC₅₀ values were calculated with an iterative nonlinear curve-fitting program (GraFit 3.0, SoftWindows).

Rat Liver Membrane AT₁ Receptor Binding Assay. Rat liver membranes were prepared according to the method of Dudley et al.³⁹ Binding of [¹²⁵I]Ang II to membranes was conducted in a final volume of 0.5 mL of 50 mM Tris-HCl (pH 7.4), supplemented with 100 mM NaCl, 10 mM MgCl₂·6H₂O, 1 mM EDTA, 0.025% bacitracin, and 0.2% BSA and containing liver homogenate corresponding to 5 mg of the original tissue weight, [¹²⁵I]Ang II (60 000 cpm, 0.027 nM), and variable concentrations of test substance. Samples were incubated at 25 °C for 1 h, and binding was terminated by filtration through Whatman GF/B glass-fiber filter sheets, using a Brandel cell harvester. The filters were washed four times with 2 mL of Tris-HCl (pH 7.4) and transferred to tubes. The radioactivity was measured in a gamma counter. Nonspecific binding was determined in the presence of 10 μ M saralasin. All experiments were performed in duplicates. K_i values were calculated using the Cheng and Prusoff equation (K_d = 0.37 nM).

Conformational Energy Calculations. The calculations of **7a**, **7b**, **8**, **27**, and **28** were performed using the Amber* all-atom force field and the all atom charge set as implemented in the program Macromodel version 5.5.⁴² The generalized Born/surface area (GB/SA) method for water developed by Still⁴¹ was used in all calculations. The number of torsion angles allowed to vary simultaneously during each Monte Carlo step ranged from 1 to $n - 1$, where n equals the total number of rotatable bonds ($n = 9$ in **7a** and **7b**, $n = 10$ in **8**, $n = 11$ in **27**, $n = 6$ in **28**). All torsion angles, except the N- and C-terminal amide bond, were defined as rotatable. Conformational searches were conducted by use of the systematic unbound multiple minimum search (SUMM) method⁶⁴ in the Batchmin program (command SPMC); 10 000 step runs were performed, and those conformations within 12 kcal/mol of the global minimum were kept. Two ring closure bonds, one for each ring, were defined for the bicyclic system. Torsional memory and geometrical preoptimization were used. Truncated Newton conjugated gradient (TNCG) minimization with a maximum of 5000 iterations was used in the conformational search with the default derivate convergence set at a value of 0.001 (kJ/mol)/Å.

Acknowledgment. We thank Anja Johansson for excellent assistance in the synthetic work, Susanna Lindman for good collaboration concerning the in vitro binding experiments on CHO cells, and the Swedish Research Council for Engineering Sciences (TFR) and the Swedish Foundation for Strategic Research (SFF) for financial support.

Supporting Information Available: ¹H and ¹³C NMR spectra for compound **12**. This material is available free of charge via the Internet at <http://pubs.acs.org>.

References

- Hruby, V. J. Conformational Restrictions of Biologically Active Peptides via Amino Acid Side Chain Groups. *Life Sci.* **1982**, *31*, 189–199.
- Toniolo, C. Conformationally Restricted Peptides through Short-Range Cyclizations. *Int. J. Pept. Protein Res.* **1990**, *35*, 287–300.
- Ball, J. B.; Alewood, P. F. Conformational Constraints: Non-peptide β -Turn Mimics. *J. Mol. Recognit.* **1990**, *3*, 55–64.
- Hölzemann, G. Peptide Conformation Mimetics. *Kontakte (Darmstadt)* **1991**, 3–12.
- Hölzemann, G. Peptide Conformation Mimetics. *Kontakte (Darmstadt)* **1991**, 55–63.
- Giannis, A.; Kolter, T. Peptidomimetics for Receptor Ligands – Discovery, Development, and Medical Perspectives. *Angew. Chem., Int. Ed. Engl.* **1993**, *32*, 1244–1267.
- Liskamp, R. M. J. Conformationally Restricted Amino Acids and Dipeptides. (Non)peptidomimetics and Secondary Structure Mimetics. *Recl. Trav. Chim. Pays-Bas* **1994**, *113*, 1–19.
- Sugg, E. E.; Dolan, C. A.; Patchett, A. A.; Chang, R. S. L.; Faust, K. A.; Lotti, V. J. Cyclic Disulfide Analogues of [Sar¹Ile⁶]angiotensin II. In *Peptides: Chemistry, Structure and Biology: Proceedings of the Eleventh American Peptide Symposium*; Rivier, J. E., Marshall, G. R., Eds.; ESCOM Publishers: Leiden, 1990; pp 305–306.
- Spear, K. L.; Brown, M. S.; Reinhard, E. J.; McMahon, E. G.; Olins, G. M.; Palomo, M. A.; Patton, D. R. Conformational Restriction of Angiotensin II: Cyclic Analogues Having High Potency. *J. Med. Chem.* **1990**, *33*, 1935–1940.
- Samanen, J.; Cash, T.; Narindray, D.; Brandeis, E.; Adams, W., Jr.; Weideman, H.; Yellin, T. An Investigation of Angiotensin II Agonist and Antagonist Analogues with 5,5-Dimethylthiazolidine-4-carboxylic Acid and Other Constrained Amino Acids. *J. Med. Chem.* **1991**, *34*, 3036–3043.
- Plucinska, K.; Kataoka, T.; Yodo, M.; Cody, W. L.; He, J. X.; Humblet, C.; Lu, G. H.; Lunney, E.; Major, T. C.; Panek, R. L.; Schelkun, P.; Skeeane, R.; Marshall, G. R. Multiple Binding Modes for the Receptor-Bound Conformations of Cyclic AII Agonists. *J. Med. Chem.* **1993**, *36*, 1902–1913.
- Matsoukas, J. M.; Hondrelis, J.; Agelis, G.; Barlos, K.; Gatos, D.; Ganter, R.; Moore, D.; Moore, G. J. Novel Synthesis of Cyclic Amide-Linked Analogues of Angiotensins II and III. *J. Med. Chem.* **1994**, *37*, 2958–2969.
- Vlahakos, D. V.; Matsoukas, J. M.; Ancans, J.; Moore, G. J.; Iliodromitis, E. K.; Marathias, K. P.; Kremastinos, D. T. Biological Activity of the Novel Cyclic Angiotensin II Analogue [Sar¹-Lys³,Glu⁵]ANG II. *Lett. Pept. Sci.* **1996**, *3*, 191–194.

- (14) Zhang, W.-J.; Nikiforovich, G. V.; Pérodin, J.; Richard, D. E.; Escher, E.; Marshall, G. R. Novel Cyclic Analogues of Angiotensin II with Cyclization between Positions 5 and 7: Conformational and Biological Implications. *J. Med. Chem.* **1996**, *39*, 2738–2744.
- (15) Schmidt, B.; Lindman, S.; Tong, W.; Lindeberg, G.; Gogoll, A.; Lai, Z.; Thörnwall, M.; Synnergren, B.; Nilsson, A.; Welch, C. J.; Sohtell, M.; Westerlund, C.; Nyberg, F.; Karlén, A.; Hallberg, A. Design, Synthesis, and Biological Activities of Four Angiotensin II Receptor Ligands with γ -Turn Mimetics Replacing Amino Acid Residues 3–5. *J. Med. Chem.* **1997**, *40*, 903–919.
- (16) Nikiforovich, G. V.; Kao, J. L.-F.; Plucinska, K.; Zhang, W.-J.; Marshall, G. R. Conformational Analysis of Two Cyclic Analogues of Angiotensin: Implications for the Biologically Active Conformation. *Biochemistry* **1994**, *33*, 3591–3598.
- (17) For other work on the bioactive conformation of Ang II, see: (a) Samanen, J. M.; Peishoff, C. E.; Keenan, R. M.; Weinstock, J. Refinement of a Molecular Model of Angiotensin II (AII) Employed in the Discovery of Potent Nonpeptide Antagonists. *Bioorg. Med. Chem. Lett.* **1993**, *3*, 909–914. (b) Joseph, M.-P.; Maigret, B.; Scheraga, H. A. Proposals for the Angiotensin II Receptor-Bound Conformation by Comparative Computer Modeling of AII and Cyclic Analogues. *Int. J. Pept. Protein Res.* **1995**, *46*, 514–526. (c) Balodis, J.; Golbraikh, A. Conformational Analysis of Cyclic Angiotensin II Analogues. *Letts. Pept. Sci.* **1996**, *3*, 195–199.
- (18) Hanessian, S.; McNaughton-Smith, G.; Lombart, H.-G.; Lubell, W. D. Design and Synthesis of Conformationally Constrained Amino Acids as Versatile Scaffolds and Peptide Mimetics. *Tetrahedron* **1997**, *53*, 12789–12854 and references therein.
- (19) Subasinghe, N. L.; Khalil, E. M.; Johnson, R. L. Stereospecific Synthesis of 2-Substituted Bicyclic Thiazolidine Lactams. *Tetrahedron Lett.* **1997**, *38*, 1317–1320.
- (20) Polyak, F.; Lubell, W. D. Rigid Dipeptide Mimics: Synthesis of Enantiopure 5- and 7-Benzyl and 5,7-Dibenzyl Indolizidinone Amino Acids via Enolization and Alkylation of δ -Oxo α,ω -Di[*N*-(9-(9-phenylfluorenyl)amino)azela] Esters. *J. Org. Chem.* **1998**, *63*, 5937–5949 and references therein.
- (21) Geyer, A.; Bockelmann, D.; Weissenbach, K.; Fischer, H. Synthesis and Structure of a Hydrophilic β -Turn Mimetic. *Tetrahedron Lett.* **1999**, *40*, 477–478.
- (22) Khalil, E. M.; Ojala, W. H.; Pradhan, A.; Nair, V. D.; Gleason, W. B.; Mishra, R. K.; Johnson, R. L. Design, Synthesis, and Dopamine Receptor Modulating Activity of Spiro Bicyclic Peptidomimetics of L-Prolyl-L-leucyl-glycinamide. *J. Med. Chem.* **1999**, *42*, 628–637.
- (23) Boatman, P. D.; Ogbu, C. O.; Eguchi, M.; Kim, H.-O.; Nakanishi, H.; Cao, B.; Shea, J. P.; Kahn, M. Secondary Structure Peptide Mimetics: Design, Synthesis, and Evaluation of β -Strand Mimetic Thrombin Inhibitors. *J. Med. Chem.* **1999**, *42*, 1367–1375.
- (24) Johannesson, P.; Lindeberg, G.; Tong, W.; Gogoll, A.; Karlén, A.; Hallberg, A. Bicyclic Tripeptide Mimetics with Reverse Turn Inducing Properties. *J. Med. Chem.* **1999**, *42*, 601–608.
- (25) Olsen, R. K.; Ramasamy, K.; Emery, T. Synthesis of N^{α},N^{δ} -Protected N^{β} -Hydroxy-L-ornithine from L-Glutamic Acid. *J. Org. Chem.* **1984**, *49*, 3527–3534.
- (26) Nahm, S.; Weinreb, S. M. *N*-Methoxy-*N*-methylamides as Effective Acylating Agents. *Tetrahedron Lett.* **1981**, *22*, 3815–3818.
- (27) Wernic, D.; DiMaio, J.; Adams, J. Enantiospecific Synthesis of L- α -Aminosuberic Acid. Synthetic Applications in Preparation of Atrial Natriuretic Factor Analogues. *J. Org. Chem.* **1989**, *54*, 4224–4228.
- (28) Barrett, A. G. M.; Pilipauskas, D. Electrochemical Oxidation of Proline Derivatives: Total Synthesis of Bulgecinine and Bulgecin C. *J. Org. Chem.* **1991**, *56*, 2787–2800.
- (29) Magnus, P.; Hulme, C. Oxidation of L-Proline Methyl Ester Derivatives with the Iodosylbenzene/Trimethylsilylazide Reagent Combination. *Tetrahedron Lett.* **1994**, *35*, 8097–8100.
- (30) Ben-Ishai, D. Reaction of Acylamino Acids with Paraformaldehyde. *J. Am. Chem. Soc.* **1957**, *79*, 5736–5738.
- (31) Holcomb, R. C.; Schow, S.; Ayrál-Kaloustian, S.; Powell, D. An Asymmetric Synthesis of Differentially Protected Meso-2,6-Diaminopimelic Acid. *Tetrahedron Lett.* **1994**, *35*, 7005–7008.
- (32) Fukuyama, T.; Liu, G.; Linton, S. D.; Lin, S.-C.; Nishino, H. Total Synthesis of (+)-Porothramycin B. *Tetrahedron Lett.* **1993**, *34*, 2577–2580.
- (33) Mueller, L. P.E.COSY, a Simple Alternative to E.COSY. *J. Magn. Reson.* **1987**, *72*, 191–196.
- (34) Braunschweiler, L.; Ernst, R. R. Coherence Transfer by Isotropic Mixing: Application to Proton Correlation Spectroscopy. *J. Magn. Reson.* **1983**, *53*, 521–528.
- (35) Bothner-By, A. A.; Stephens, R. L.; Lee, J.; Warren, C. D.; Jeanloz, R. W. Structure Determination of a Tetrasaccharide: Transient Nuclear Overhauser Effects in the Rotating Frame. *J. Am. Chem. Soc.* **1984**, *106*, 811–813.
- (36) Wüthrich, K. *NMR of Proteins and Nucleic Acids*; John Wiley & Sons: New York, 1986.
- (37) Perlman, S.; Schambye, H. T.; Rivero, R. A.; Greenlee, W. J.; Hjorth, S. A.; Schwartz, T. W. Non-Peptide Angiotensin Agonist. *J. Biol. Chem.* **1995**, *270*, 1493–1496.
- (38) CHO cells stably expressing the rat AT₁ receptor were generously provided by Prof. Thue Schwartz, University Department of Clinical Biochemistry, Rigshospitalet, Copenhagen, Denmark.
- (39) Dudley, D. T.; Panek, R. L.; Major, T. C.; Lu, G. H.; Bruns, R. F.; Klinkefus, B. A.; Hodges, J. C.; Weishaar, R. E. Subclasses of Angiotensin II Binding Sites and Their Functional Significance. *Mol. Pharmacol.* **1990**, *38*, 370–377.
- (40) Kataoka, T.; Beusen, D. D.; Clark, J. D.; Yodo, M.; Marshall, G. R. The Utility of Side-Chain Cyclization in Determining the Receptor-Bound Conformation of Peptides: Cyclic Tripeptides and Angiotensin II. *Biopolymers* **1992**, *32*, 1519–1533.
- (41) Still, W. C.; Tempczyk, A.; Hawley, R. C.; Hendrickson, T. Semianalytical Treatment of Solvation for Molecular Mechanics and Dynamics. *J. Am. Chem. Soc.* **1990**, *112*, 6127–6129.
- (42) Mohamadi, F.; Richards, N. G. J.; Guida, W. C.; Liskamp, R.; Lipton, M.; Caufield, C.; Chang, G.; Hendrickson, T.; Still, W. C. MacroModel-An Integrated Software System for Modeling Organic and Bioorganic Molecules Using Molecular Mechanics. *J. Comput. Chem.* **1990**, *11*, 440–467.
- (43) Lewis, P. N.; Momany, F. A.; Scheraga, H. A. Chain Reversals in Proteins. *Biochim. Biophys. Acta* **1973**, *303*, 211–229.
- (44) Richardson, J. S. The Anatomy and Taxonomy of Protein Structure. *Adv. Protein Chem.* **1981**, *34*, 167–399. We searched for the classical β -turn types by allowing $\pm 30^\circ$ deviation from the ideal Φ and Ψ values.
- (45) Wilmot, C. M.; Thornton, J. M. Analysis and Prediction of the Different Types of β -Turn in Proteins. *J. Mol. Biol.* **1988**, *203*, 221–232.
- (46) Cornille, F.; Fobian, Y. M.; Slomczynska, U.; Beusen, D. D.; Marshall, G. R.; Moeller, K. D. Anodic Amide Oxidations: Conformationally Restricted Peptide Building Blocks from the Direct Oxidation of Dipeptides. *Tetrahedron Lett.* **1994**, *35*, 6989–6992.
- (47) Cornille, F.; Slomczynska, U.; Smythe, M. L.; Beusen, D. D.; Moeller, K. D.; Marshall, G. R. Electrochemical Cyclization of Dipeptides toward Novel Bicyclic, Reverse-Turn Peptidomimetics. 1. Synthesis and Conformational Analyses of 7,5-Bicyclic Systems. *J. Am. Chem. Soc.* **1995**, *117*, 909–917.
- (48) Slomczynska, U.; Chalmers, D. K.; Cornille, F.; Smythe, M. L.; Beusen, D. D.; Moeller, K. D.; Marshall, G. R. Electrochemical Cyclization of Dipeptides to Form Novel Bicyclic, Reverse-Turn Peptidomimetics. 2. Synthesis and Conformational Analysis of 6,5-Bicyclic Systems. *J. Org. Chem.* **1996**, *61*, 1198–1204.
- (49) Baldwin, J. E.; Hulme, C.; Schofield, C. J.; Edwards, A. J. Synthesis of Potential β -Turn Bicyclic Dipeptide Mimetics. *J. Chem. Soc., Chem. Commun.* **1993**, 935–936.
- (50) Botti, P.; Pallin, D.; Tam, J. P. Cyclic Peptides from Linear Unprotected Peptide Precursors through Thiazolidine Formation. *J. Am. Chem. Soc.* **1996**, *118*, 10018–10024.
- (51) Hodges, J. C.; Hamby, J. M.; Blankley, C. J. Angiotensin II Receptor Binding Inhibitors. *Drugs Future* **1992**, *17*, 575–593.
- (52) Cordopatis, P.; Manessi-Zoupa, E.; Theodoropoulos, D.; Bossé, R.; Bouley, R.; Gagnon, S.; Escher, E. Methylation in Positions 1 and 7 of Angiotensin II. *Int. J. Pept. Protein Res.* **1994**, *44*, 320–324.
- (53) Matsoukas, J. M.; Bigam, G.; Zhou, N.; Moore, G. J. ¹H NMR Studies of [Sar¹]Angiotensin II Conformation by Nuclear Overhauser Effect Spectroscopy in the Rotating Frame (ROESY): Clustering of the Aromatic Rings in Dimethyl sulfoxide. *Peptides* **1990**, *11*, 359–366.
- (54) Zhou, N.; Moore, G. J.; Vogel, H. J. Proton NMR Studies of Angiotensin II and Its Analogues in Aqueous Solution. *J. Protein Chem.* **1991**, *10*, 333–343.
- (55) Hondrelis, J.; Matsoukas, J.; Agelis, G.; Cordopatis, P.; Zhou, N.; Vogel, H.; Moore, G. J. ¹H NMR Conformational Studies in Water of Angiotensin II Analogues Modified at the N- and C-termini: Interactions of the Aromatic Side Chains and Folding of the N-terminal Domain. *Collect. Czech. Chem. Commun.* **1994**, *59*, 2523–2532.
- (56) Matsoukas, J. M.; Agelis, G.; Wahhab, A.; Hondrelis, J.; Panagiotopoulos, D.; Yamdagni, R.; Wu, Q.; Mavroumoustakos, T.; Maia, H. L. S.; Ganter, R.; Moore, G. J. Differences in Backbone Structure between Angiotensin II Agonists and Type I Antagonists. *J. Med. Chem.* **1995**, *38*, 4660–4669 and references therein.
- (57) Adlington, R. M.; Baldwin, J. E.; Catterick, D.; Pritchard, G. J. A Versatile Approach to Pyrimidin-4-yl Substituted α -Amino Acids from Alkynyl Ketones: The Total Synthesis of L-Lathyrine. *J. Chem. Soc., Chem. Commun.* **1997**, 1757–1758.

- (58) Collado, I.; Ezquerra, J.; Vaquero, J. J.; Pedregal, C. Diastereoselective Functionalization of 5-Hydroxy Prolinates by Tandem Horner-Emmons-Michael Reaction. *Tetrahedron Lett.* **1994**, *35*, 8037–8040.
- (59) Lee, B. H.; Miller, M. J. Constituents of Microbial Iron Chelators. The Synthesis of Optically Active Derivatives of δ -N-Hydroxy-L-ornithine. *Tetrahedron Lett.* **1984**, *25*, 927–930.
- (60) Bold, G.; Steiner, H.; Moesch, L.; Walliser, B. Herstellung von 'Semialdehyd'-Derivaten von Asparaginsäure und Glutaminsäure durch *Rosenmund*-Reduktion. *Helv. Chim. Acta* **1990**, *73*, 405–410.
- (61) Gelb, M. H.; Lin, Y.; Pickard, M. A.; Song, Y.; Vederas, J. C. Synthesis of 3-Fluorodiaminopimelic Acid Isomers as Inhibitors of Diaminopimelate Epimerase: Stereocontrolled Enzymatic Elimination of Hydrogen Fluoride. *J. Am. Chem. Soc.* **1990**, *112*, 4932–4942.
- (62) Babievskii, K. K.; Belikov, V. M.; Belokon, Y. N. Amino Acids. Communication 2. Synthesis of DL-Proline from Nitroacetic Ester Derivatives. *Bull. Acad. Sci. USSR, Div. Chem. Sci. Engl. Transl.* **1965**, *5*, 1188–1190.
- (63) Satterthwait, A. C., Jr.; Arrhenius, T.; Chiang, L.-C.; Cabeza, E. Patent WO 93/21206.
- (64) Goodman, J. M.; Still, W. C. An Unbounded Systematic Search of Conformational Space. *J. Comput. Chem.* **1991**, *12*, 1110–1117.

JM991089Q